CHAPTER 4
CRITICAL ANALYSIS OF THE NUMERICAL MODELLING

We will use two different models of behavior for the soil. The first uses a law of Mohr Coulomb, and the second uses the Mohr Coulomb Model with softening. The first modeling gathers 3 various simulations, with several calculations for each simulation by using various mechanical properties and geometrical. The second modeling gathers 2 various simulations.

4.1 Analyzes with the model of Mohr-Coulomb

In this part, we will analyze and compare the various results of the Mohr Coulomb Model. We have 2 systems which have the same geometry of the soil (low height) with the various shapes of cavity (circle and ellipse), and another system of great dimension.

4.1.1 Earth dam - low height with circular cavity

We take the results of the γp according to the coefficient of reduction (R) (*Cref = 300kPa*). The results for each model (a rayon of the cavity given and several values of cohesion) are given according to the maximum value of γp (in zones not belonging to the vault) present in the system.
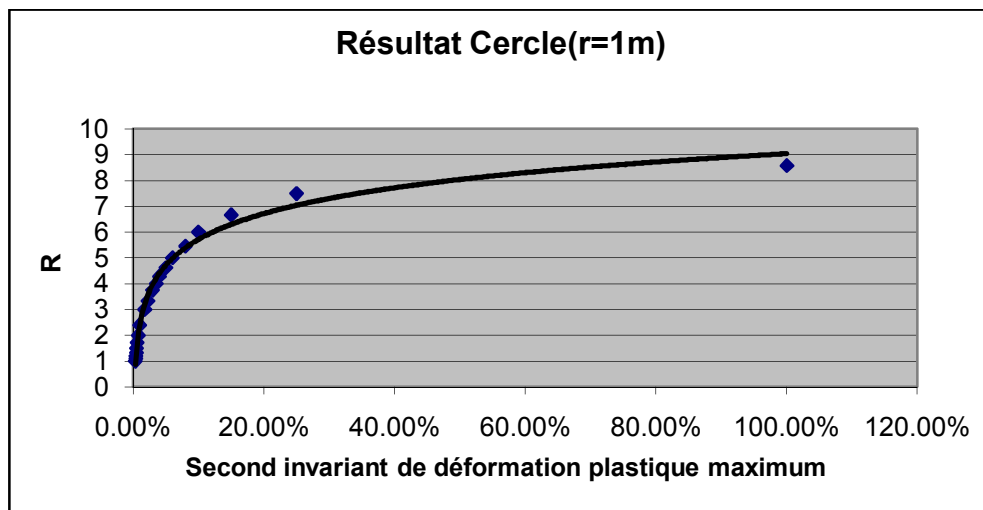
Figure 34 Mohr Coulomb Model with circular cavity (r=1m)

Résultat Cercle(r=5m)
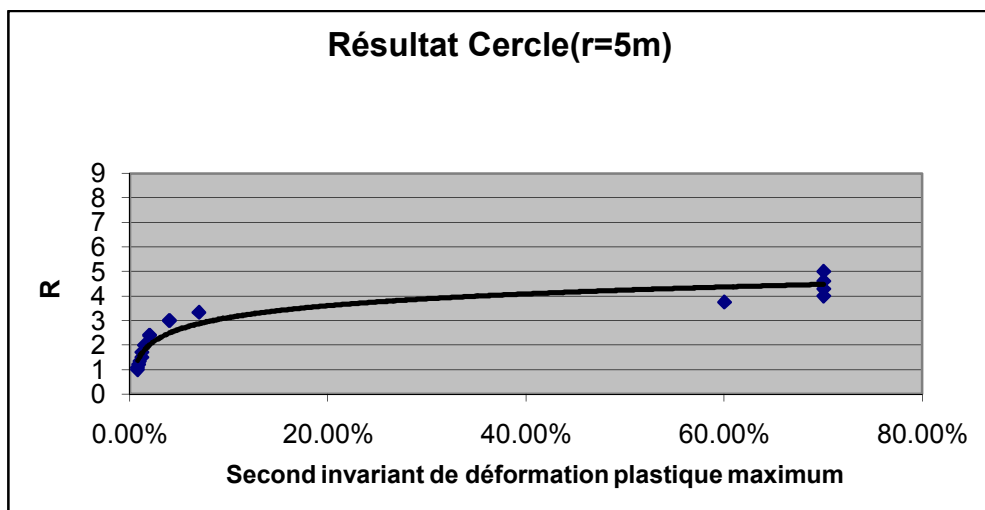
Figure 35 Mohr Coulomb Model with circular cavity (*r=5m*)

Résultat Cercle(r=9m)
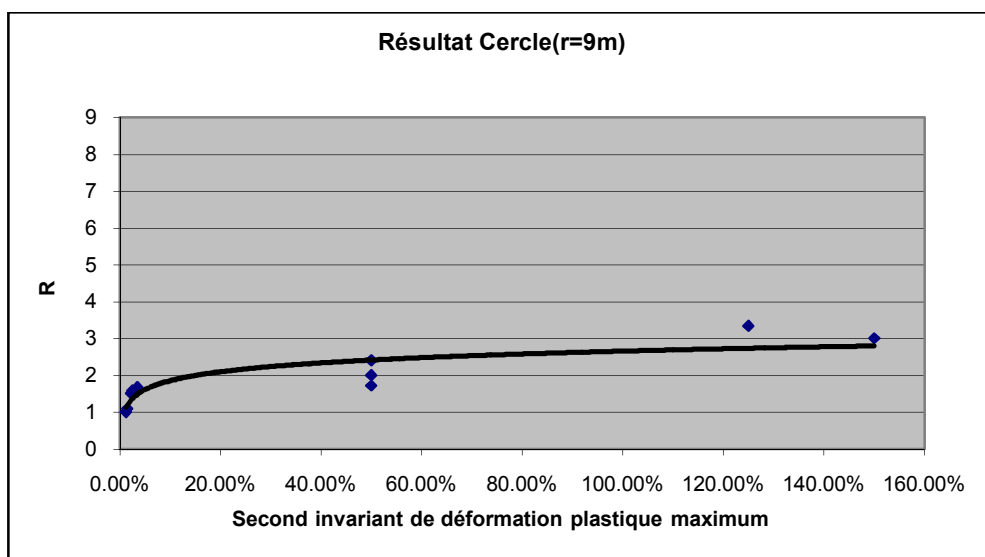
Figure 36 Mohr Coulomb Model with circular cavity (*r=9m*)

We summarize the results on Table 9,

Table 9 Result of the Mohr Coulomb Model with circular cavity

Height of the Model - H (m)	10					
Rayon - R (m)	1	2	3	4	5	9
Maximum coefficient of reduction - R_{max}	8.57	6.70	5.73	4.81	4.14	2.33
Limiting cohesion - C_{lim}; γ^p=5% (kPa)	65	70	80	87	97	179
Ultimate cohesion - C_{ult} (kPa)	35	45	52	62	72	129
γ^p_{max} (%)	100	60	70	80	70	50

We note that the geometry of the cavity has an important effect on the evolution of the second invariant of the plastic deformations maximum (γpmax). The enlarging of the circular cavity cause a drop in the value of the maximum coefficient of reduction. When the cavity is large, we need a value of larger cohesion undrained to ensure the stability of the system. This is well checked with the value of the ultimate cohesion which increases (and Rmax decreases) when the rayon increases (Figure 37).
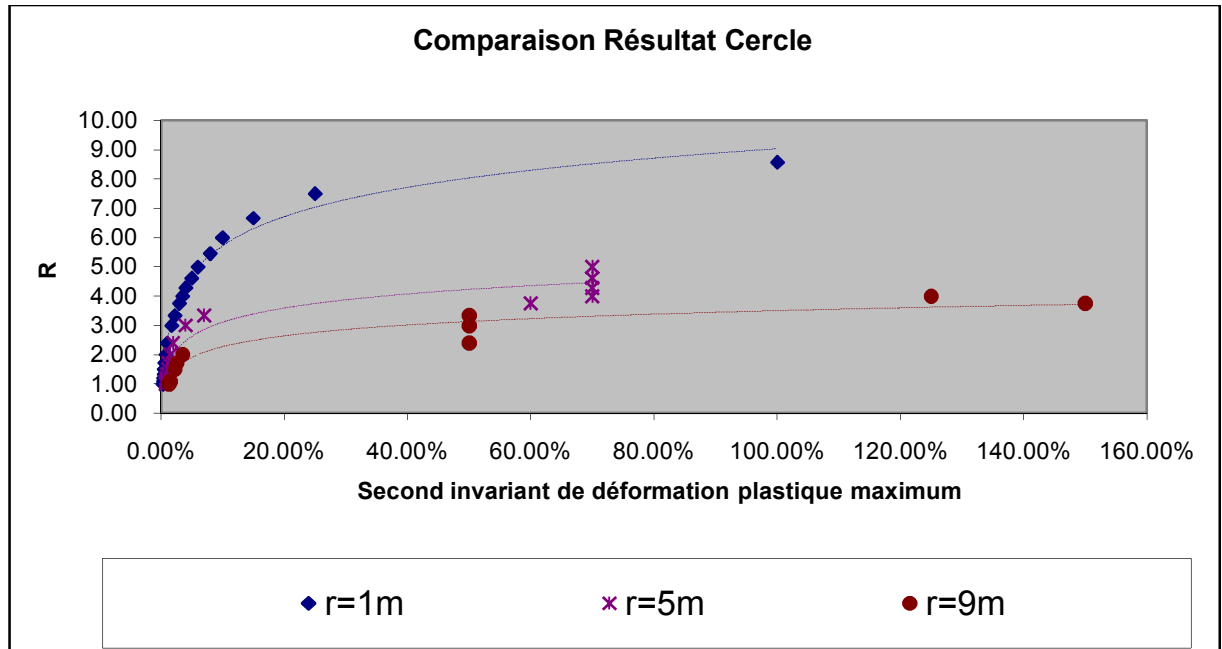

Figure 37 Comparison between the Mohr Coulomb Model and circular cavity

Figure 38 shows the distribution of γ^p_{max} in the Mohr Coulomb Model low height when γ^p is larger than 5%. We thus have a total rupture. The model has a cohesion of the soil of 80 kPa and a rayon of the cavity of 5m with a height of the earth dam of 10m. γ^p goes up to 60%, but in the pictorial display, we restricted the representation with 10% to see exactly where the great deformations are located.

JOB TITLE : SSI (1% - 10%)

FLAC (Version 5.00)

LEGEND

12-Jun-09 10:37
step   197980
-1.389E+00 <x< 2.639E+01
-1.901E+01 <y< 8.765E+00

Max. shear strain increment
  0.00E+00
  2.00E-02
  4.00E-02
  6.00E-02
  8.00E-02
  1.00E-01
Contour interval= 1.00E-02

Marciela esa DEWA
Stagiaire ECL
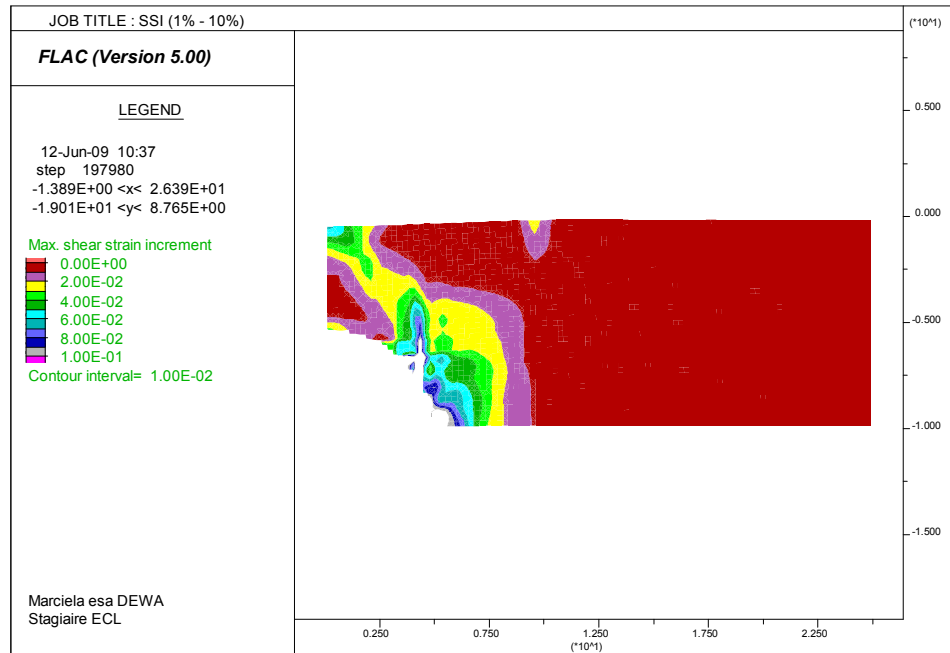
Figure 38 Presentation of γp with total rupture, circular model MC cavity (*r=5m; C=80kPa*)

By using the index of plasticity and the speed of deformation which are reproduced on Figure 39, Figure 40 & Figure 41, the phenomenon of collapse is shown more clearly.

JOB TITLE : L'indice de plasticité (r=5m;Cu=80kPa)

FLAC (Version 5.00)

LEGEND

12-Jun-09 10:37
step 197980
-1.389E+00 <x< 2.639E+01
-1.901E+01 <y< 8.765E+00

Plasticity Indicator
* at yield in shear or vol.
X elastic, at yield in past
o at yield in tension
Attached Gridpoints
Boundary plot

0   5E 0

Marciela esa DEWA
Stagiaire ECL
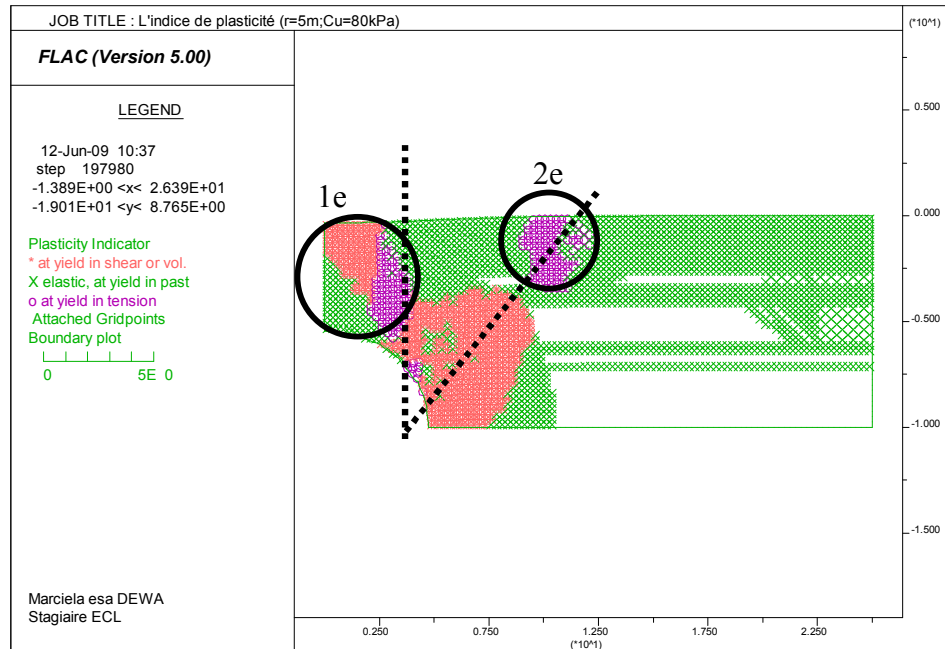
Figure 39 Index of plasticity of the Mohr-Coulomb model in low height (*r=5m, Cu=80kPa*)

JOB TITLE : Les vecteurs de vitesse (r=5m;Cu=80kPa)

FLAC (Version 5.00)

LEGEND

12-Jun-09 10:37
step 197980
-1.389E+00 <x< 2.639E+01
-1.901E+01 <y< 8.765E+00

Velocity vectors
max vector = 3.199E-05

0   1E -4

Boundary plot

0   5E 0

Marciela esa DEWA
Stagiaire ECL
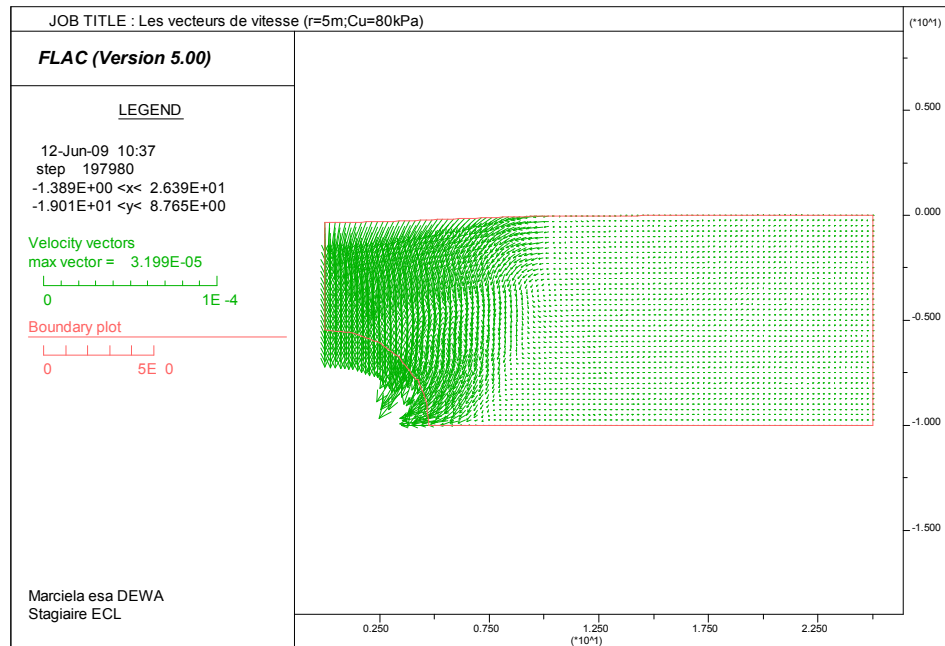
Figure 40 Vectors speed of the Mohr Coulomb Model in low height (*r=5m, Cu=80kPa*)
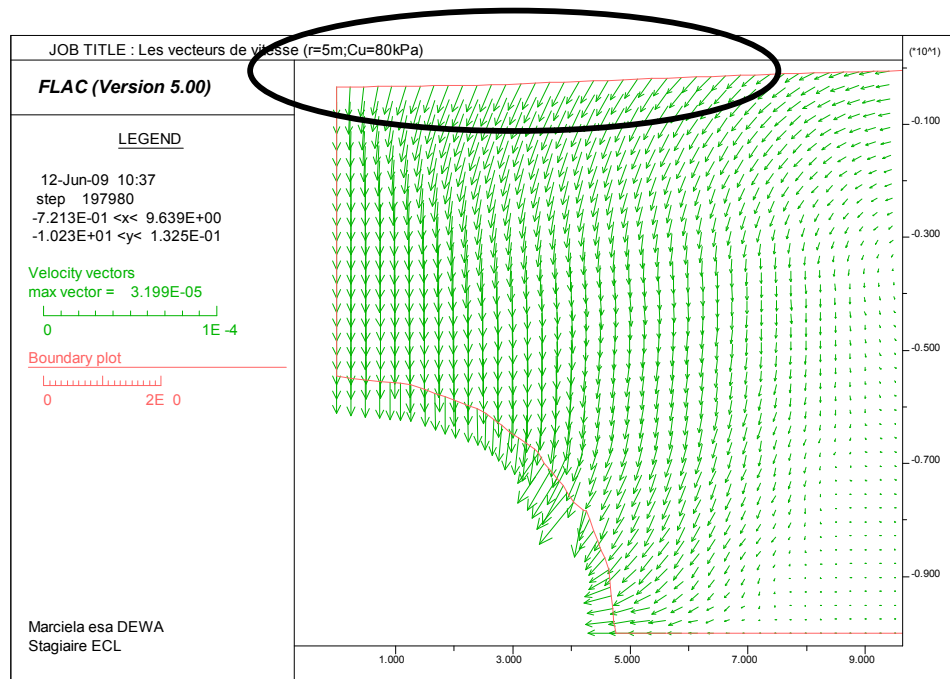
Figure 41 Zoom of the vectors speed of the Mohr Coulomb Model in low height (*r=5m, Cu=80kPa*)

We notice that collapse being shown by the vectors speed starts with the angle of 30-45° (axis X). On the other hand, if we look at the surface of the soil to the vertical axis (3rd circle on Figure 41), we can say the vertical part falling down, which mean the vertical rupture happens. The zone of plasticity (Figure 39) shows us the same result for the vertical rupture.

Moreover if we look at the second circle on Figure 39, we remark that there is a second rupture just beside the first one. To see this type of collapse, it is necessary to give a higher value of R than the R used (either for example with a cohesion of 55 kPa) (Figure 42)
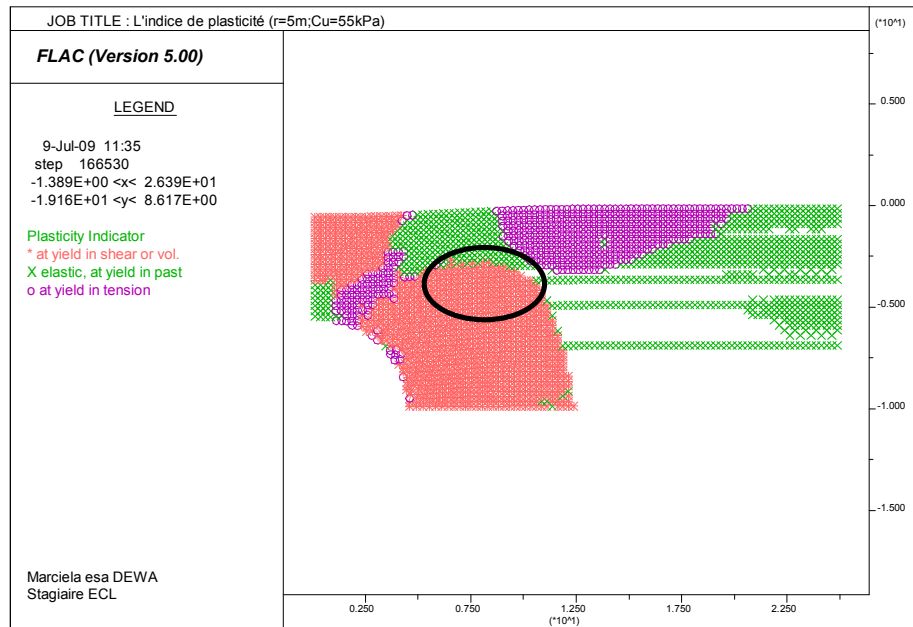
Figure 42 Index of plasticity for the basic model (Mohr-*Coulomb, r=5m, Cu=55kPa*)

The model above uses a lower cohesion of 55 kPa. And we note that the slip of the soil in direction of cavity is marked. In order to conclude this assumption, we consider other results in displacement in X and Y (Figure 43 and Figure 44), the vectors speed (Figure 45).
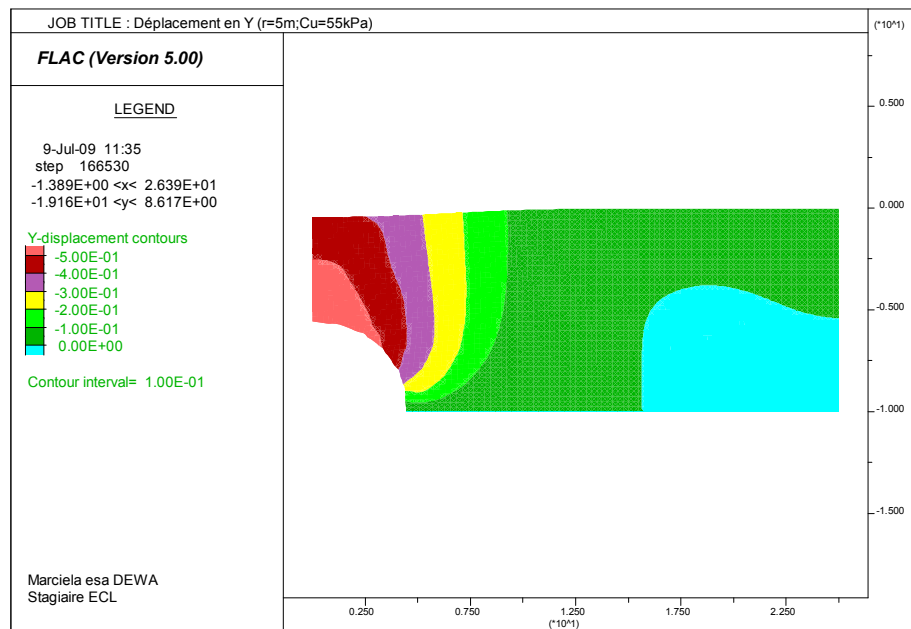
**Figure 43 Displacement in Y of the Mohr Coulomb Model in low height (*r=5m, Cu=55kPa*)**
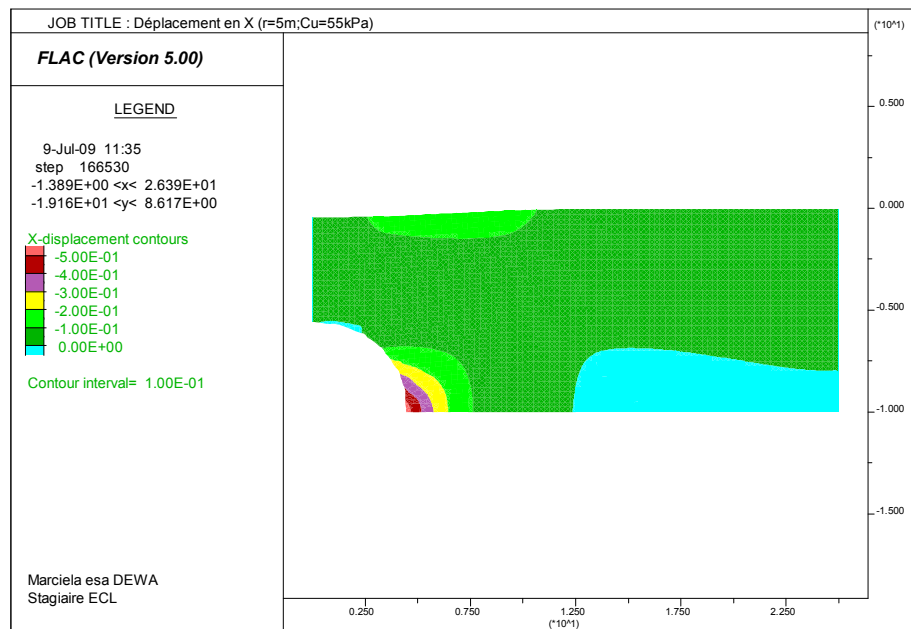
Figure 44 Displacement in X of the Mohr Coulomb Model in low height (*r=5m, Cu=55kPa*)

```
JOB TITLE : Vecteurs de vitesse (r=5m;Cu=55kPa)          (*10^1)

FLAC (Version 5.00)

     LEGEND

   9-Jul-09 11:35
  step  166530
 -6.740E-01 <x< 1.326E+01
 -1.281E+01 <y< 1.124E+00

 Velocity vectors
 max vector =  6.572E-04

    0            2E -3

 Marciela esa DEWA
 Stagiaire ECL
```
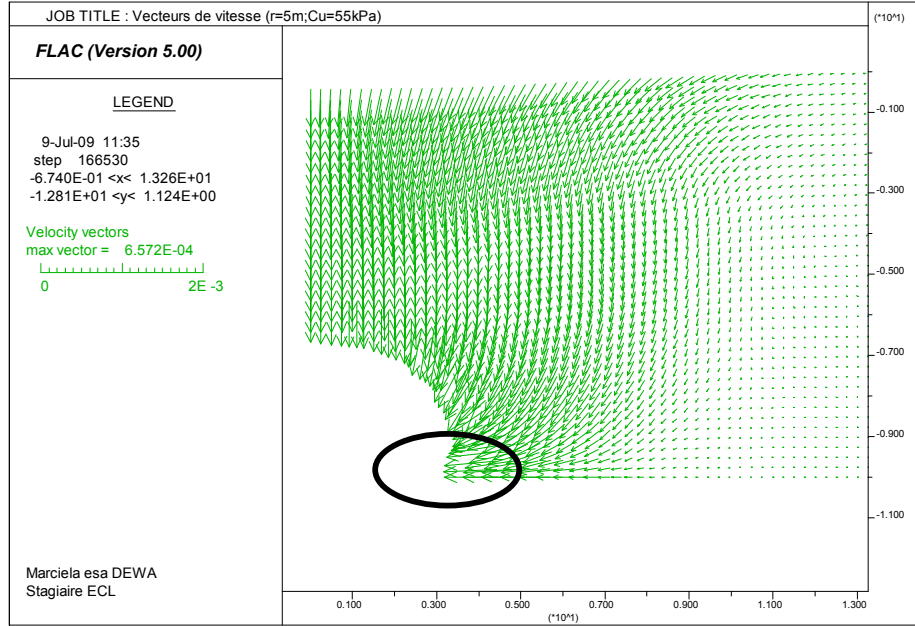
Figure 45 Vectors speed of the Mohr Coulomb Model in low height (*r=5m, Cu=55kPa*)

We note that the mode of rupture occurs vertically by subsidence to the top of the cavity. The stability of the zone where the rupture is likely to occur is ensured by the soil which did not reach its plastic limit yet (see Figure 42).

The vectors speed on Figure 45 show us that there is also an important effect according to the horizontal axis (circle).

This study shows clearly that the formation process of a breach starting from a conduit is done in two times: initially it there with the subsidence to the top of the conduit, then there is formation of a slip forming a slope on the level of the breach.
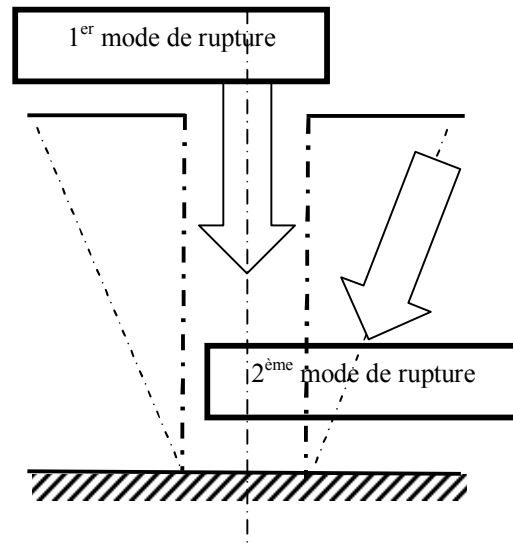
Figure 46 Mode of rupture during the widening of a con-

4.1.2 *Earth dam - low height with elliptic cavity*

The results, which we obtain with the model of Mohr Coulomb and a circular cavity, show that the geometry has important effects in the evolution of collapse. This model wants to prove the effect of the geometry. (For the model with an elliptic cavity, $C_{ref} = 1300kPa$).
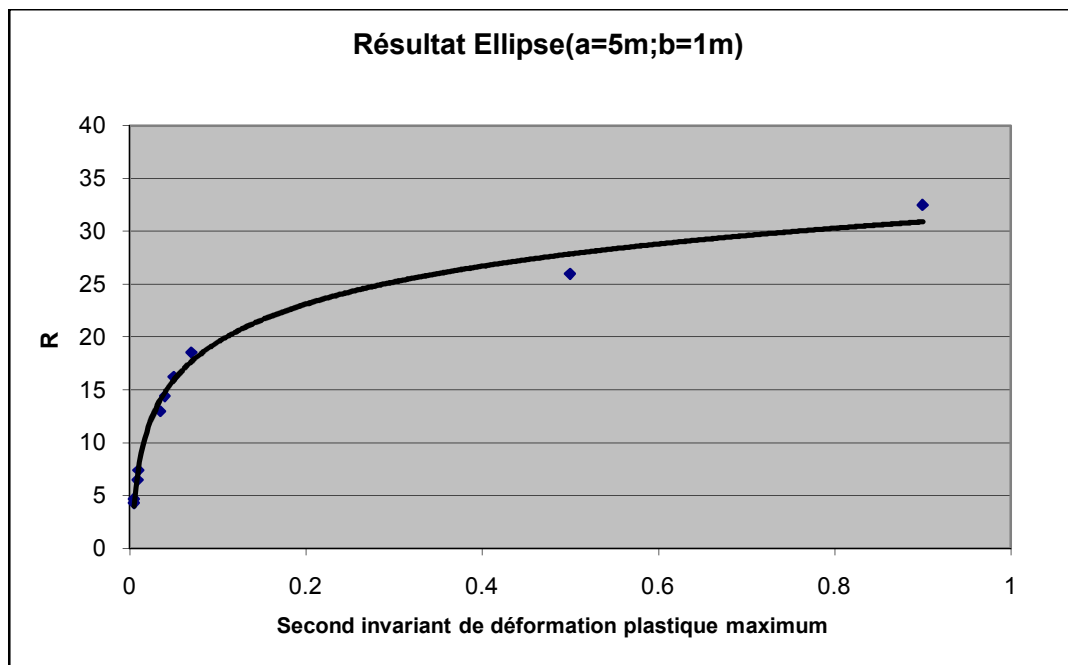

**Figure 47 Model of Mohr Coulomb with an elliptic cavity (*a=5m b=1m*)**
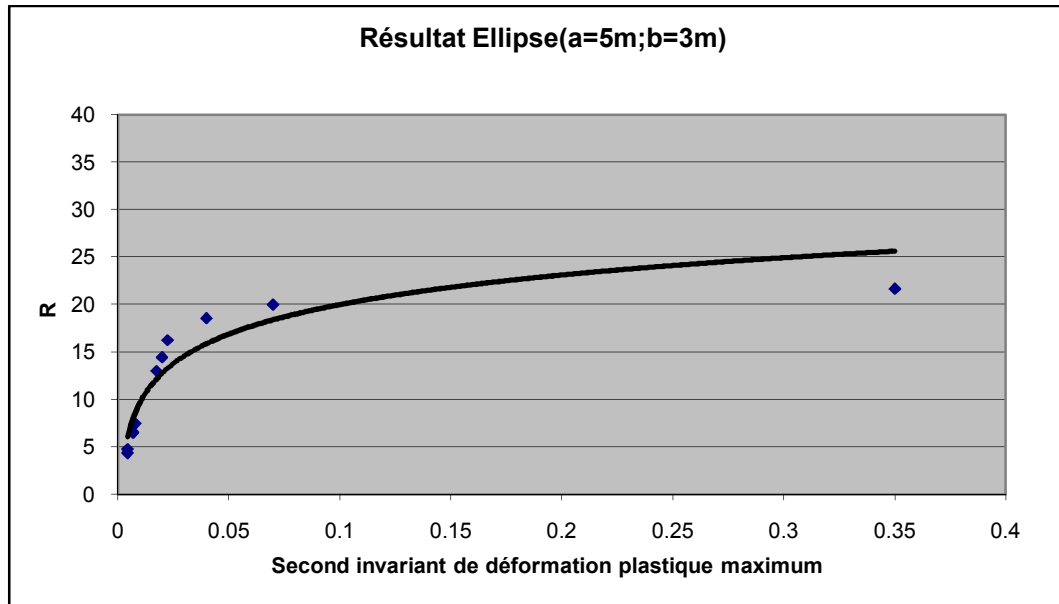
Figure 48 Model of Mohr Coulomb with an elliptic cavity (*a=5m b=3m*)

Table 10 Result of the Model of Mohr Coulomb with an elliptic cavity (*Cu=1300kPa*)

Height of the model - h (m)	10									
Height - a (m)	1		3		5		9			
Width - b (m)	3	5	1	5	1	3	1	3	5	7
Maximum coefficient of reduction - R_{max}	21.67	13.33	26.67	13.72	25.67	21.67	13.72	18.57	16	14.44
Limiting cohesion - C_{lim}; γ^p=5% (kPa)	120	800	70	150	80	67	140	126	130	150
Ultimate cohesion - C_{ult} (kPa)	60	124	49	95	51	60	95	70	81	90
γ^p_{max} (%)	70	75	50	47	50	35	80	125	150	150

Based on Fgure 47 ; Figure 48 ; and Figure 35, We can compare the effect of geometry. The maximum values for coefficient of reduction (R_{max}) for the three models are,

- model $A=5m$ ellipse*; B=1m* → R_{max} *=25.67*

- model $A=5m$ ellipse*; B=3m* → R_{max} *=21.67*

- circular model $A=B=5m$ → R_{max} *=4.14 (Cu=300kPa)*→ R_{max} *=17,94*

We note that the conduit with elliptic cavity is much more stable than the model with circular cavity. This is explained by the weight of the roof to the top of the cavity which is larger in the model with circular cavity.

We compare the various results (γ^p and the vectors speed) for the three models, to see the evolution of collapse.
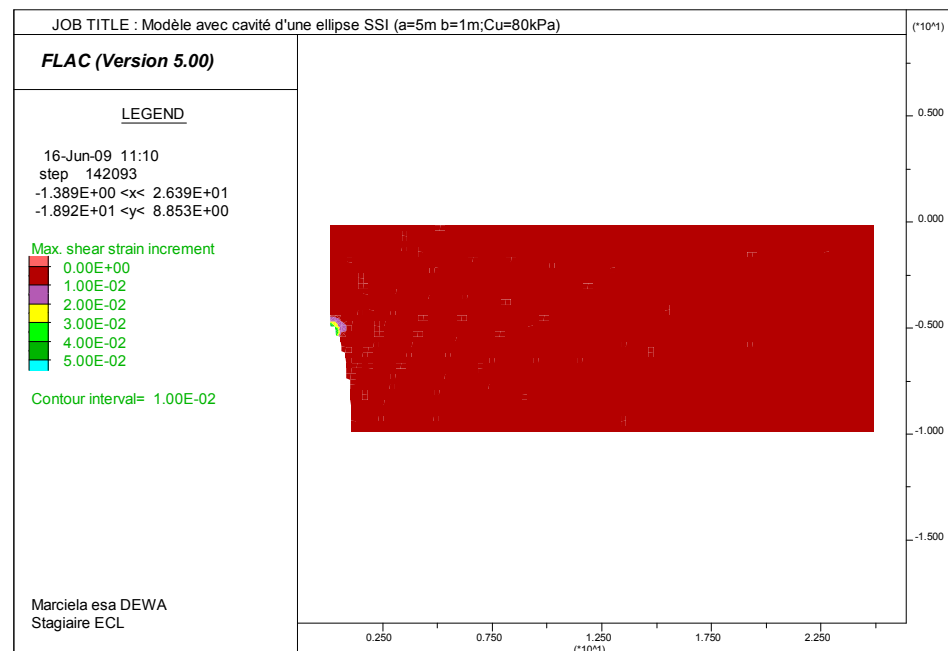

**Figure 49 Presentation of γp, elliptic model MC cavity (*a=5m b=1m*; *C=80kPa*)**
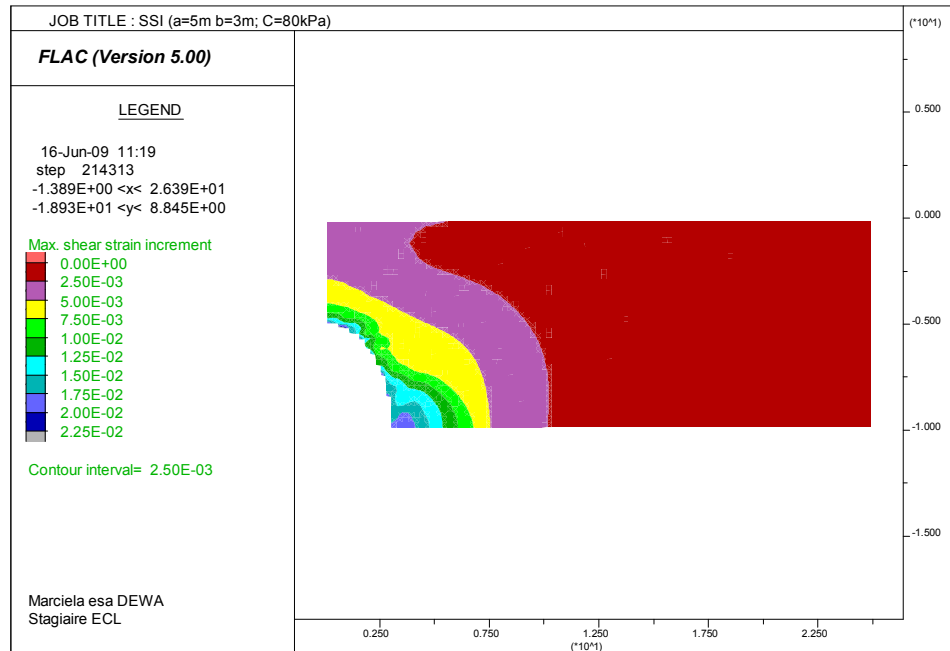
Figure 50 Presentation of γp, elliptic model MC cavity (*a=5m b=3m*; *C=80kPa*)
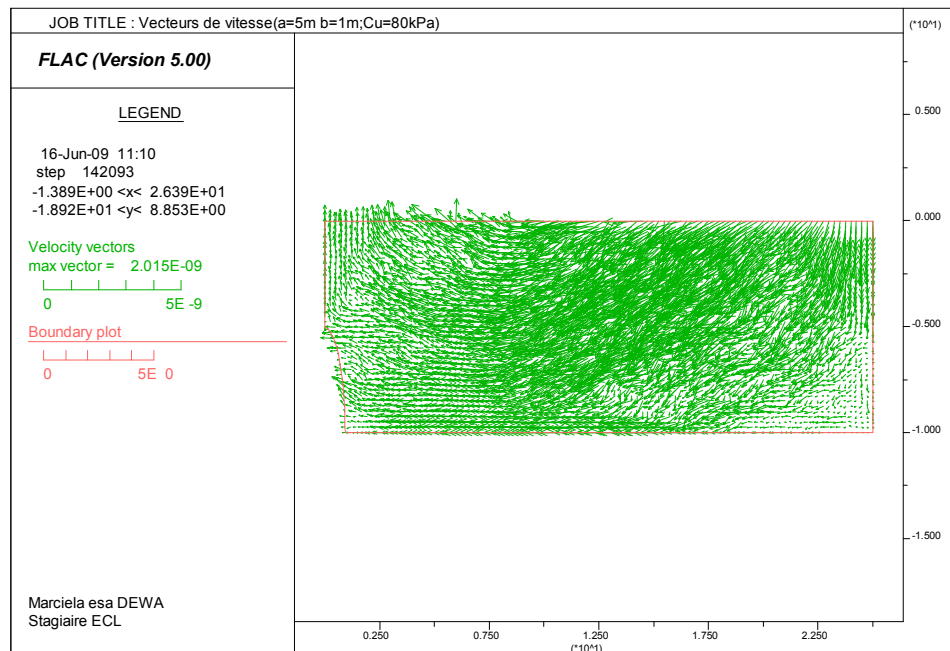
Figure 51 Vectors of speed, model MC with elliptic cavity (*a=5m, b=1m, Cu=80kPa*)
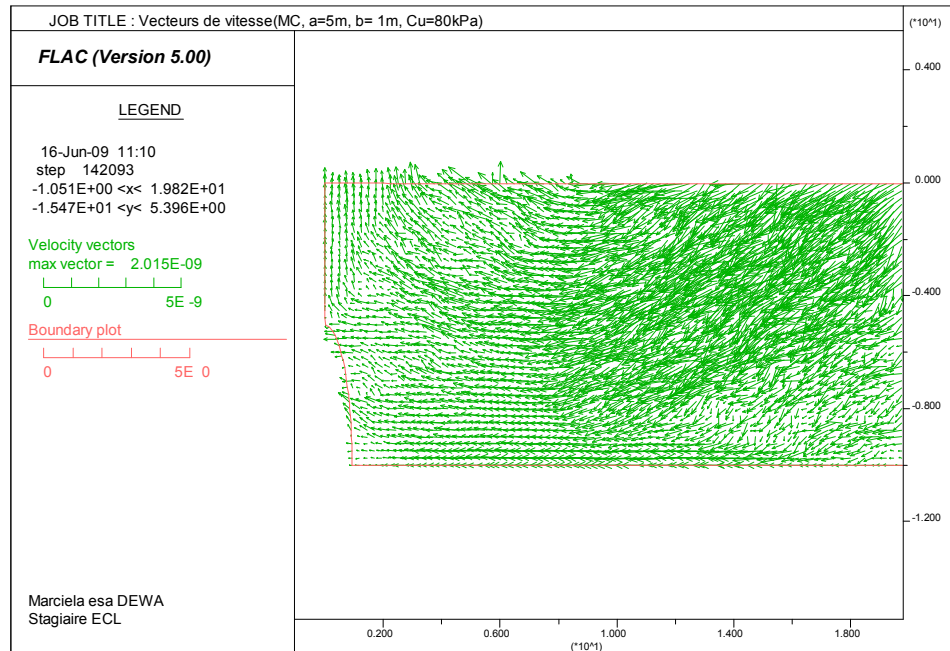
Figure 52 Vectors of speed refined, model MC with elliptic cavity (*a=5m, b=1m, Cu=80kPa*)
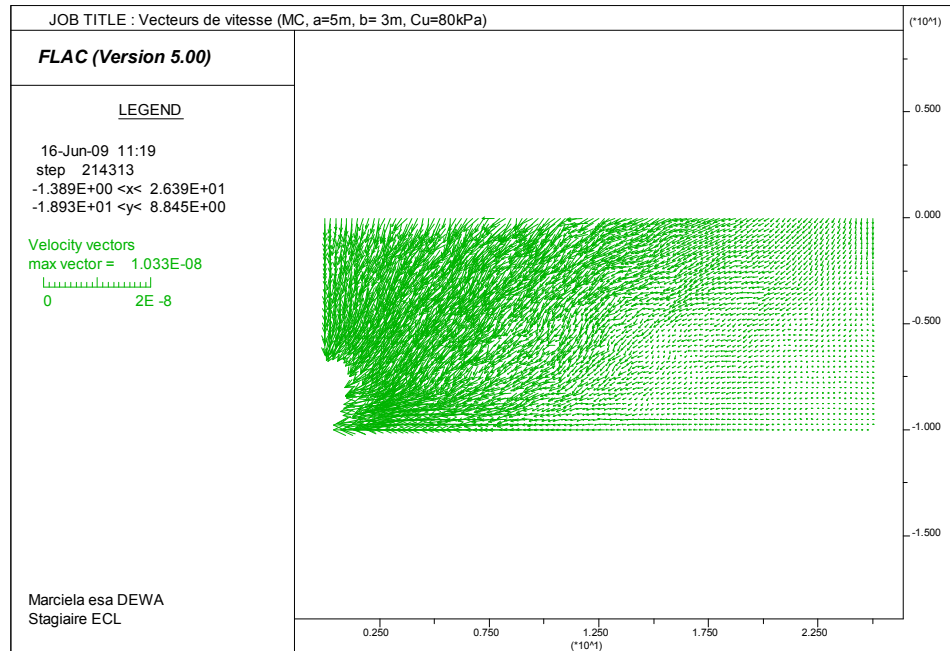
**Figure 53 Vectors of speed, model MC with elliptic cavity (*a=5m, b=3m, Cu=80kPa*)**
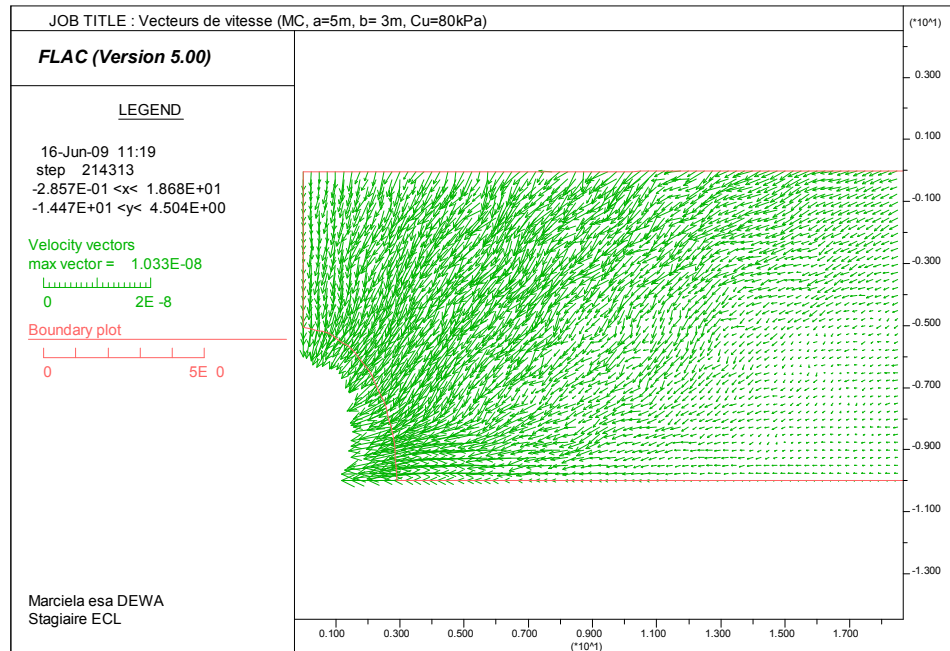
**Figure 54 Vectors of speed refined, model MC with elliptic cavity (*a=5m, b=3m, Cu=80kPa*)**
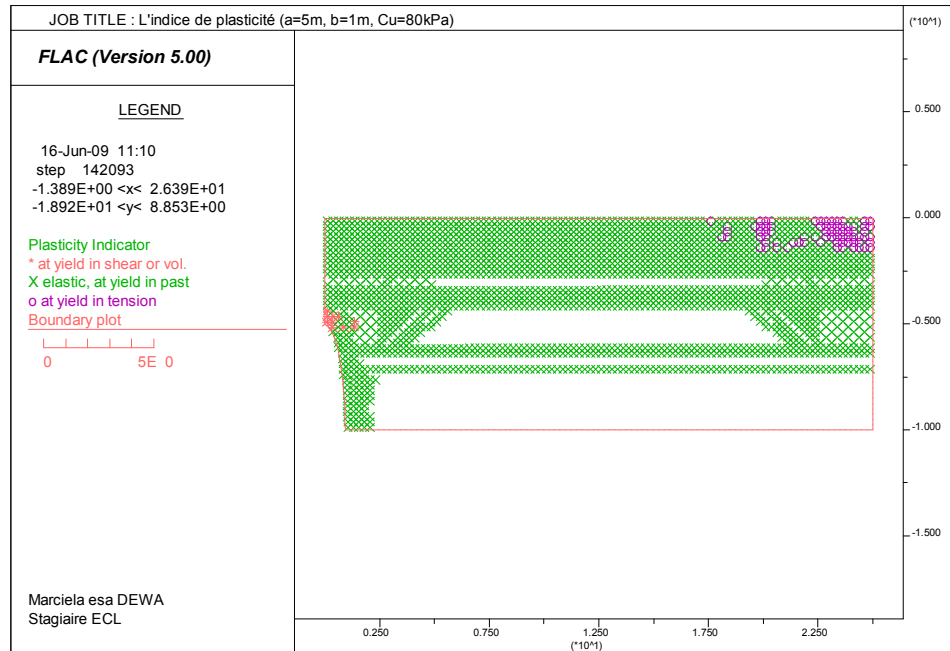
**Figure 55 Index of plasticity, model MC with elliptic cavity (*a=5m, b=1m, Cu=80kPa*)**
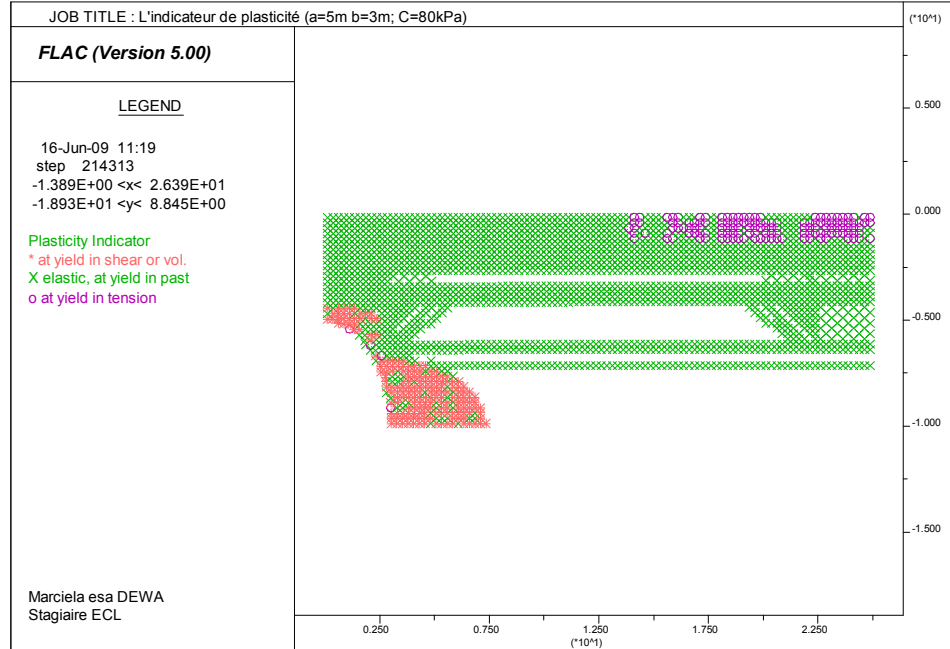
Figure 56 Index of plasticity, model MC with elliptic cavity (*a=5m, b=3m, Cu=80kPa*)

By comparing the result in the case of an earth dam with the same mechanical behavior, we notice the effects of the change of the geometry of cavity. The stability of the soil is also affected by the shape of cavity.

An important remark on the shape of cavity is R_{max} which does not evolve in the same way as γ^p_{max}. In the former model with a circular cavity, R_{max} evolved just as the values of γ^p_{max}. At the time the cavity is larger, R_{max} and the γ^p_{max} drop (because we need a value of stronger cohesion, which makes R lower).

It is not only the case for the cavity of an ellipse. Let us take the case of *Cu=80 kPa* with a cavity having the height, *a=5m*, where the γ^p changes 5% to 2,25%. The enlarging in width does not increase γ^p_{max}, but it decreases it (case of A5B1 and A5B3, decreases by 5% to 2,25%).

- o model *A=5m* ellipse*; B=1m; Cu=80kPa*   ➔ γ^p_{max}=5%

- o model *A=5m* ellipse*; B=3m; Cu=80kPa*   ➔ γ^p_{max}=2,25%

- o circular model *A=B=5m; Cu=80kPa*   ➔ γ^p_{max}=60%

This assumption lets us to predict different modes of rupture (see Figure 58 and Figure 59).
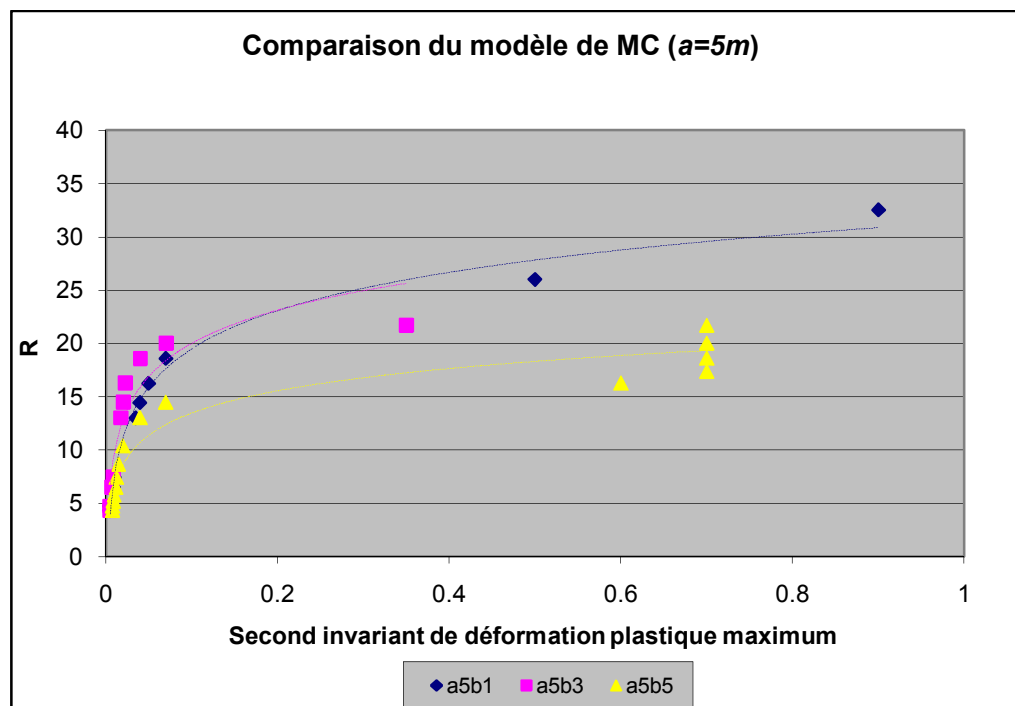
**Figure 57 Comparison with different form of the geometry of cavity (*Cref=1300kPa*)**
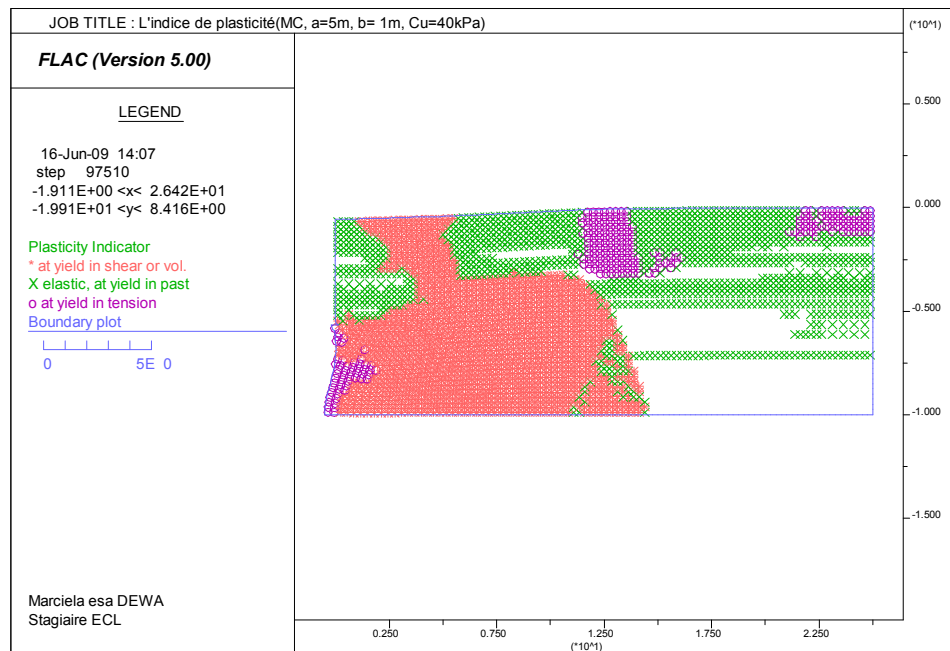
Figure 58 Index of plasticity, model MC with elliptic cavity (*a=5m, b= 1m, Cu=40kPa*)
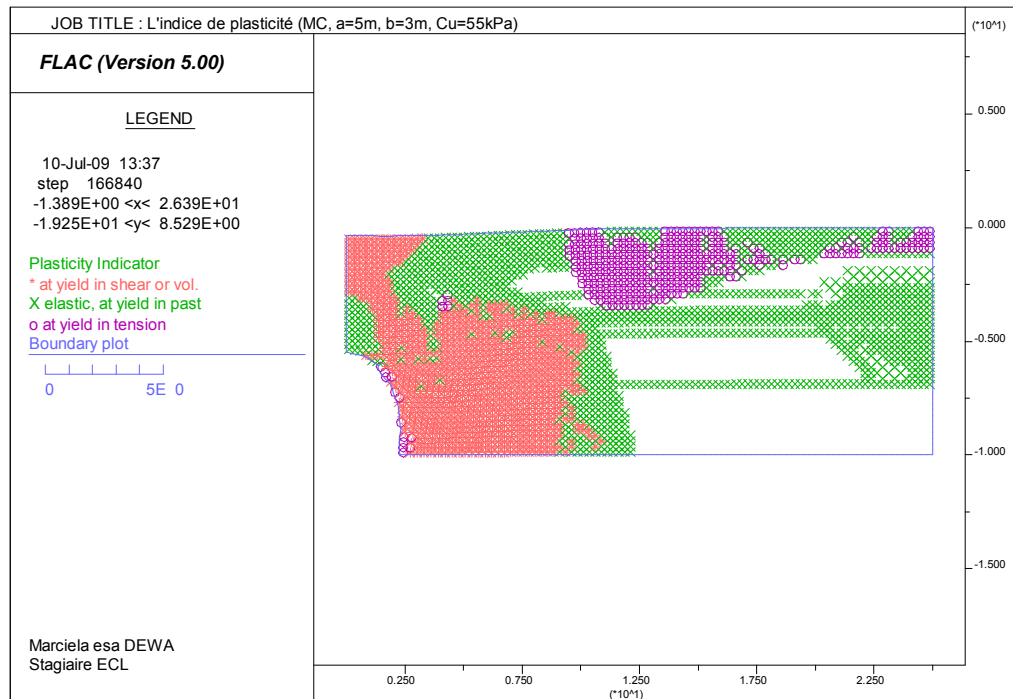
Figure 59 Index of plasticity, model MC with elliptic cavity (*a=5m, b=3m, Cu=55kPa*)

Let us take the case with the width (*b)* is fixed. The curve of comparison is shown on this figure
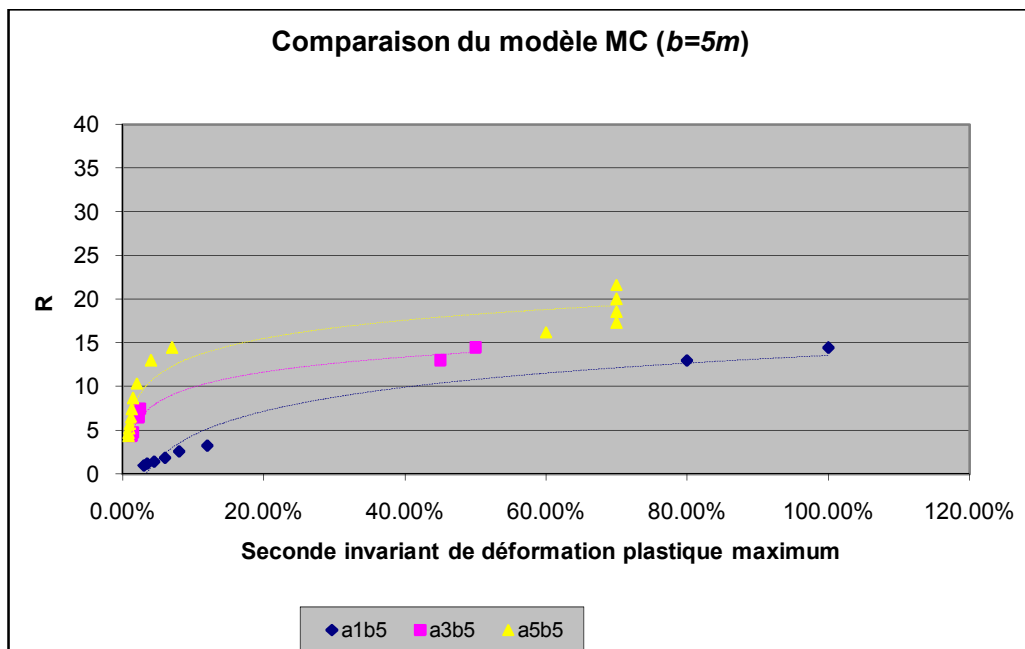
Figure 60 Comparison with different form of the geometry of cavity (flattened model; *Cref=1300kPa*)

Based on the coefficient of reduction (R), the circular cavity is more stable than the flattened elliptic cavity. The ultimate cohesion used for the model with flattened elliptic cavity is larger than the model with circular cavity. For better analyzing, we take the two cases in the curve (a=1m; B =5m) and (a=3m; b=5m).
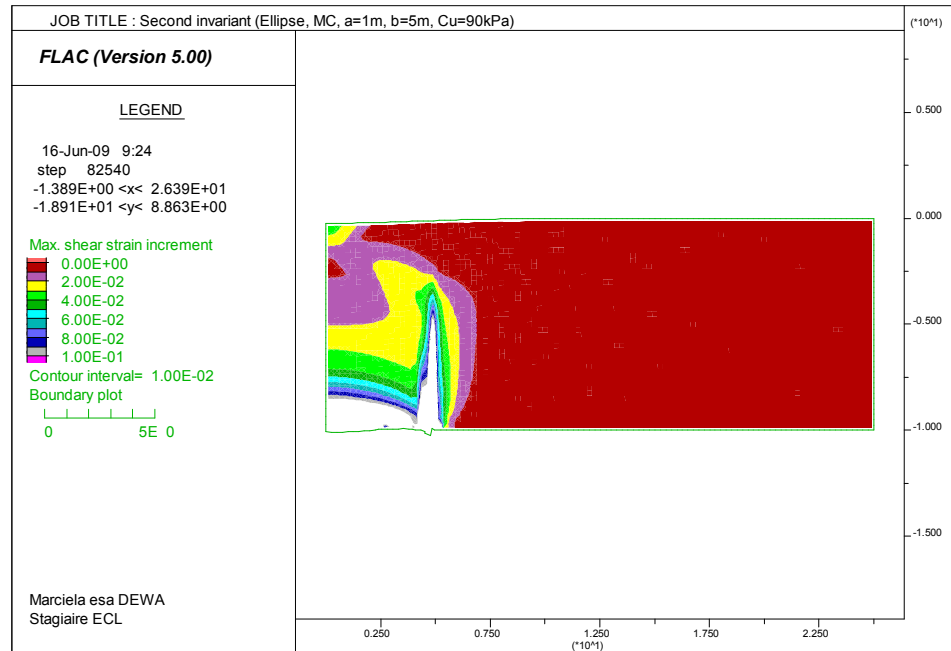
**Figure 61 Presentation of γp, model MC with elliptic cavity (*a=1m b=5m*; *C=90kPa*)**
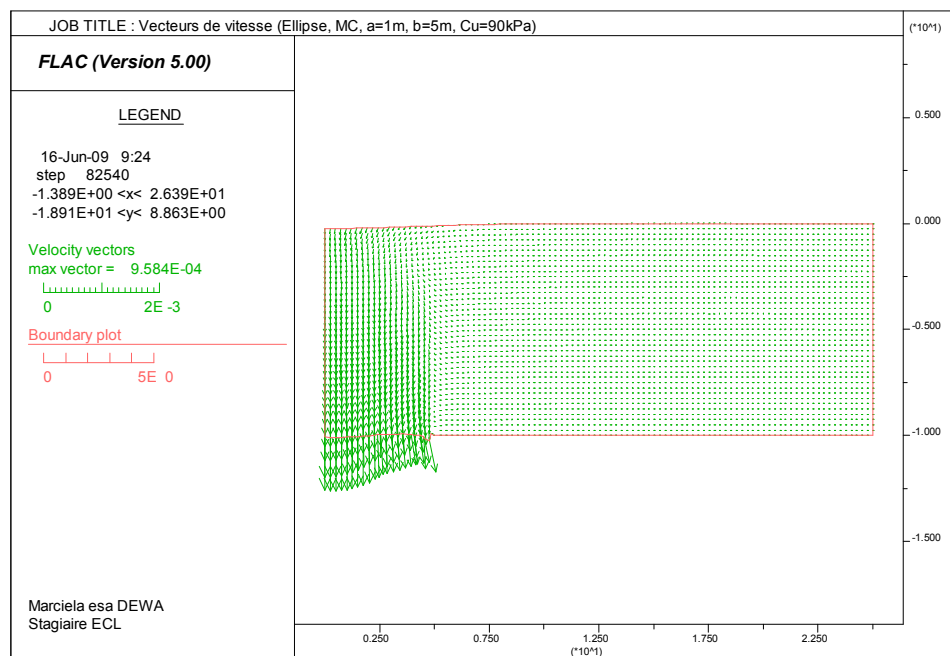
**Figure 62 Vectors of speed, model MC with elliptic cavity (*a=1m, b=5m, Cu=90kPa*)**
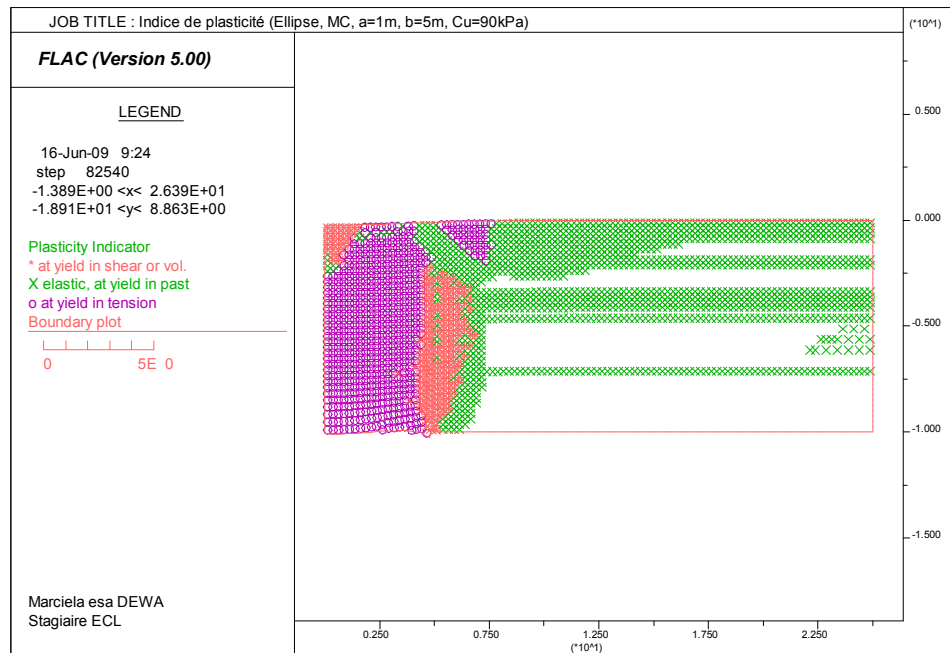
**Figure 63 Index of plasticity, model MC with elliptic cavity (*a=1m, b=5m, Cu=90kPa*)**
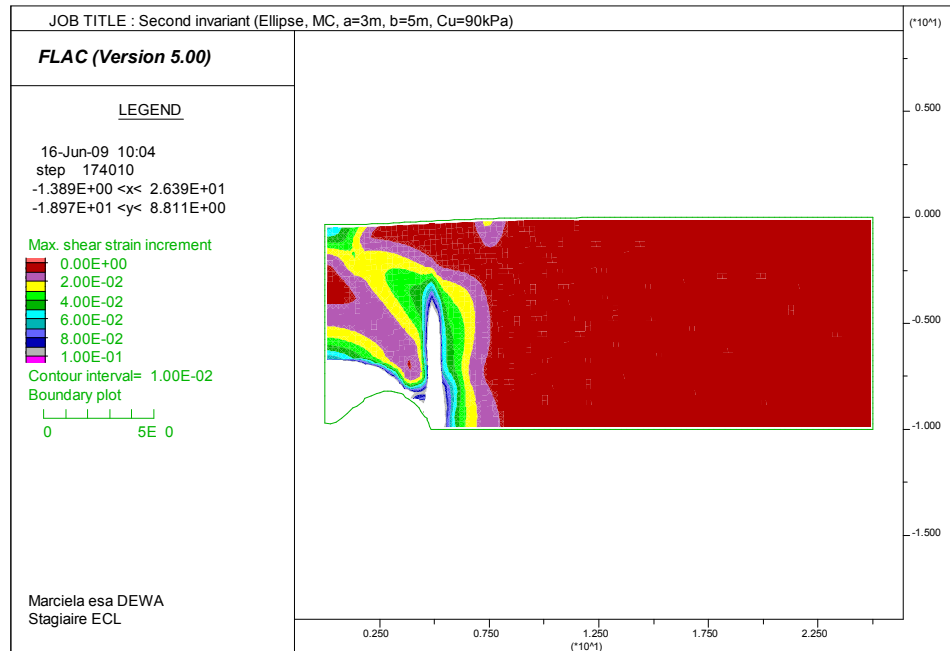
Figure 64 Presentation of γp, elliptic model MC cavity (*a=1m b=3m*; *C=90kPa*)
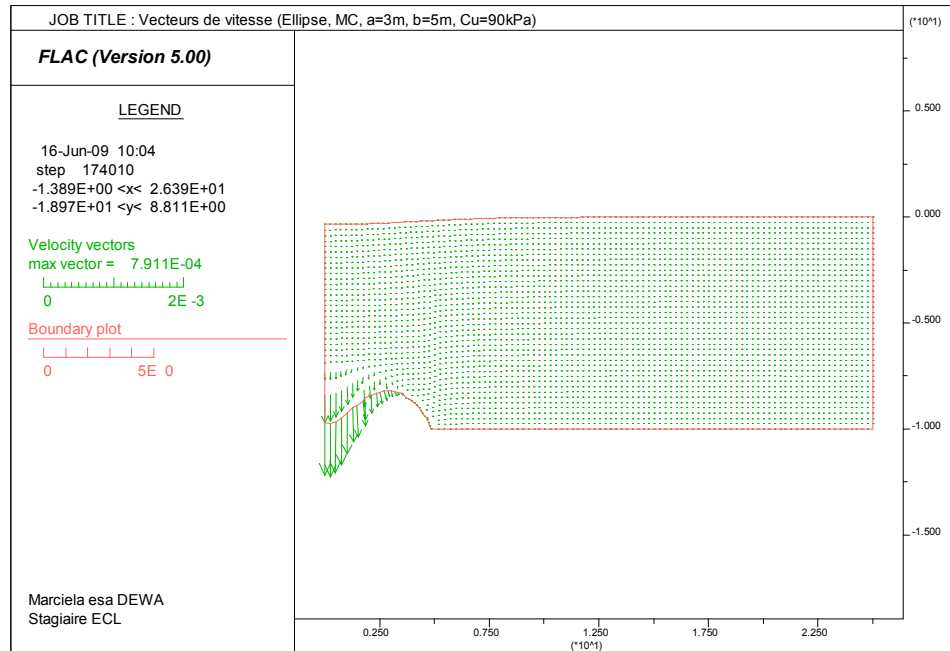

**Figure 65 Vectors of speed, Model MC with elliptic cavity (*a=3m, b=5m, Cu=90kPa*)**
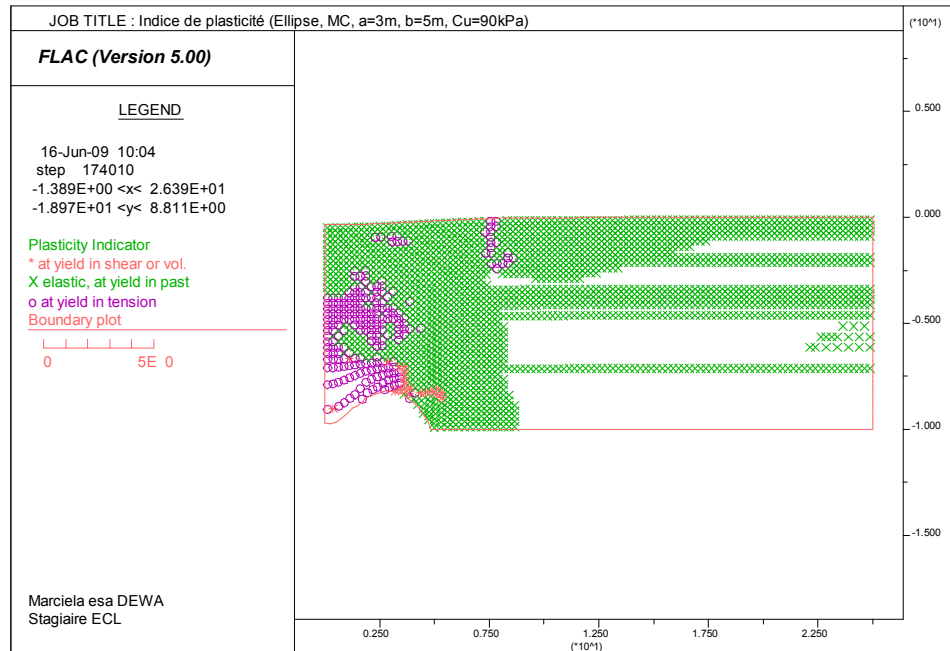
Figure 66 Index of plascticity, Model MC with elliptic cavity (*a=3m, b=5m, Cu=90kPa*)

Figure 63 shows us the total collapse of the earth dam when the cavity having the shape of a flattened ellipse. It is the opposite of the preceding result where collapse occurs if the cavity is sufficiently large and close to surface. On the other hand for the less flattened elliptic cavity (case of a=3m, b=5m; Figure 66), we note that there will be a starter of rupture with depression on the surface. This phenomenon is happens because of the weight of the soil on the top of the roof of cavity. Total collapse is likely to occur when the weight of the soil on the top of the roof of conduit is too big.

To conclude, we will compare the number of stability for each model according to its enlarging: either in height, or in width.

Comparaison du nombre de stabilité, modèle ellipse (A=5m ou B=M)
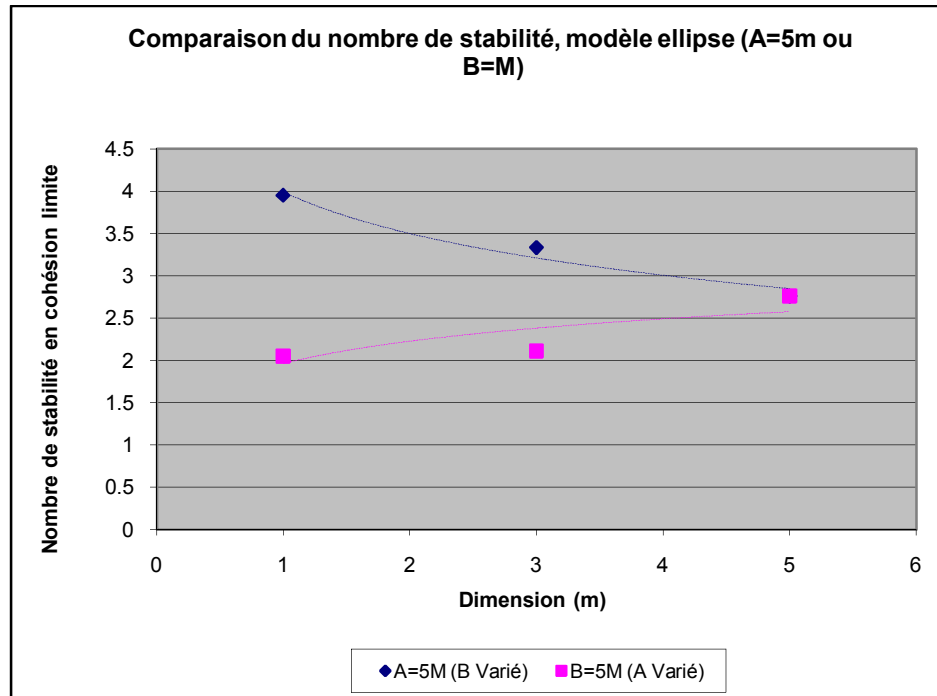
Figure 67 Comparison between number of stability and various models

We note on Figure 67, which the model having a cavity in ellipse with a height larger than its width (case of A5B1) is much more stable than the model having a larger width (case of A1B5).

4.1.3 Earth dam - great height with circular cavity

The effect of the enlarging of the dimension of the earth dam (thus an increase height of the earth dam) will be analyzed on this model. (We use $C_{ref}=2700kPa$ for the model having a height of 30m and $C_{ref}=5000kPa$ for the model having a height of 90m) (Table 11)

Table 11 Mohr Coulomb Model in great height

Height of the Model - h (m)	30					90						
Rayon - r (m)	1	3	9	18	27	1	5	9	18	27	54	81
Maximum coefficient of reduction - R_{max}	30	27	13.5	6.5	3.75	25	21	12.5	8.33	5.88	3.33	2
Limiting cohesion - C_{lim}; γ^p=5% (kPa)	190	225	270	380	750	450	550	680	750	850	1700	3500
Ultimate cohesion - C_{ult} (kPa)	90	100	200	415	720	200	238	400	600	850	1501	2500
γ^p_{max} (%)	125	80	17.5	3.25	45	60	80	25	12	5	5	2

The results which we obtain here cannot be compared directly with the model of Mohr Coulomb of low height earth dam, because the geometry is different. We then propose to make a comparison with its number of stability.

Table 12 Number of stability based in cohesion limits (height of the model of 10m)

Rayon/Height	0.1	0.2	0.3	0.4	0.5	0.9
N_{lim}	3.08	2.86	2.5	2.35	2.11	1.14

Table 13 Number of stability based in cohesion limits (height of the model of 30m)

Rayon/Height	0.03	0.1	0.3	0.6	0.9
N_{lim}	3.16	2.67	2.22	1.58	0.8

Table 14 Number of stability based in cohesion limits (height of the model of 90m)

Rayon/Height	0.01	0.05	0.1	0.2	0.3	0.6	0.9
N_{lim}	4	3.27	2.65	2.4	2.12	1.06	0.51

**Comparaison de nombre de stabilité (Cohésion limite)**
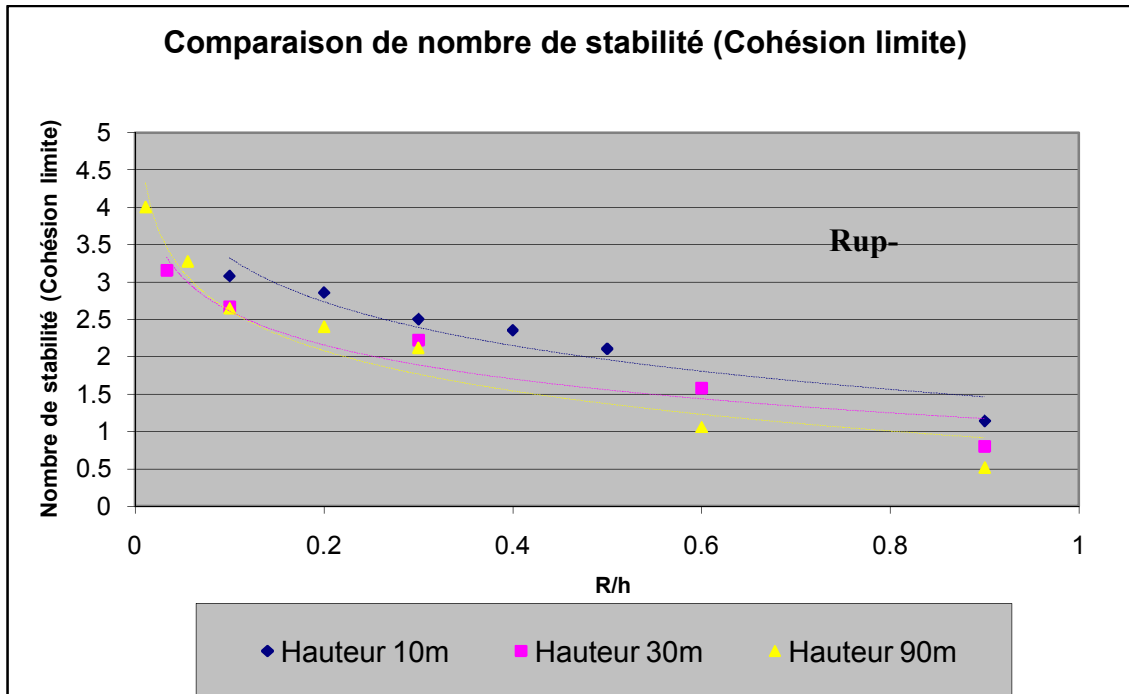
Figure 68 Comparison of the number of stability based in cohesion limits (model of 10m, 30m, 90m)

Table 15 Number of stability based in ultimate cohesion (height of the model of 10m)

Rayon/Height	0.1	0.2	0.3	0.4	0.5	0.9
N_{ult}	5.71	4.47	3.82	3.20	2.76	1.55

Table 16 Number of stability based in ultimate cohesion (height of the model of 30m)

Rayon/Height	0.03	0.1	0.3	0.6	0.9
N_{ult}	6.67	6	3	1.44	0.83

Table 17 Number of stability based in ultimate cohesion (height of the model of 90m)

Rayon/Height	0.01	0.05	0.1	0.2	0.3	0.6	0.9
N_{ult}	9	7.56	4.5	2.99	2.12	1.19	0.60

**Comparaison de nombre de stabilité (Cohésion ultime)**
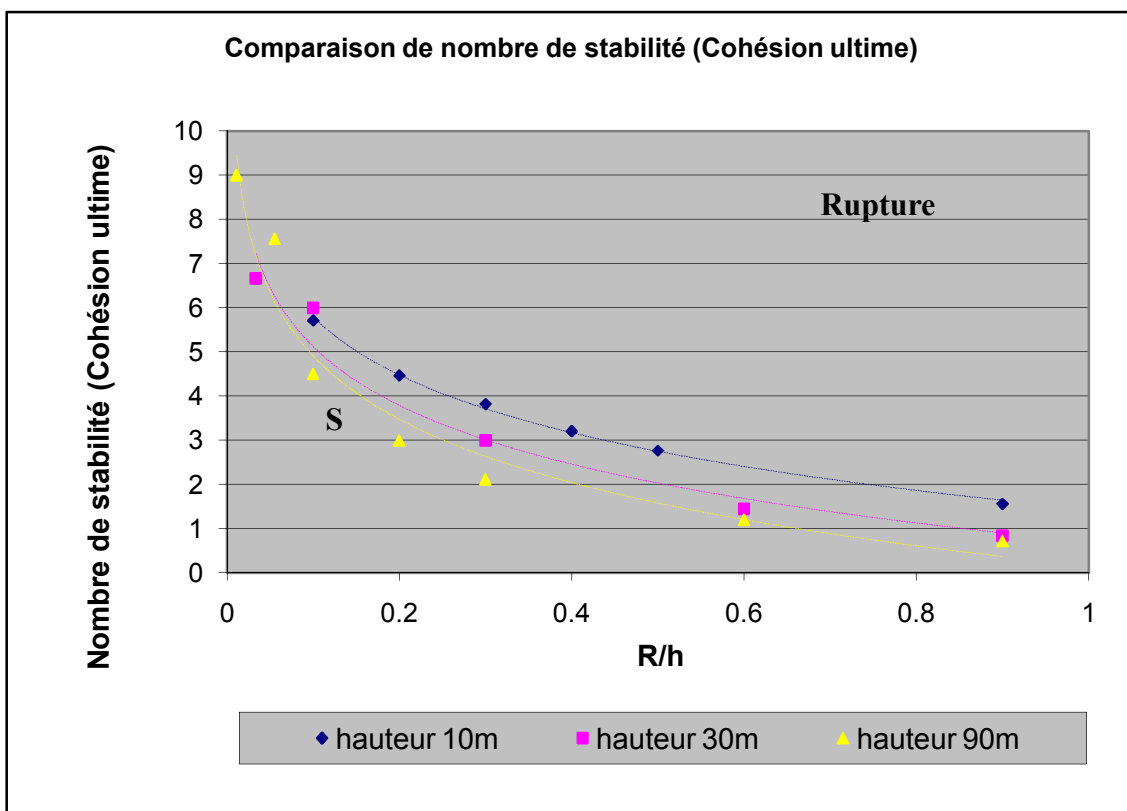
Figure 69 Comparison of the number of stability based in ultimate cohesion (model of 10m, 30m, 90m)

According to Figure 69, the three models tend to have the same curve of stability when the ratio rayon/height (*r/h*) is small. When the cavity is large, where that it approaches surface, the number of stability drops. Moreover the earth dam great height is less stable than the earth dam low height.

For more detailed analysis, we take the case of a cavity with a rayon of the circular cavity of 27m for the two types of heights (30m and 90m). This rayon of cavity enables us to see the two evolutions of collapse when the cavity is close to surface (case of a earth dam of 30m) and far from surface (case of a earth dam of 90m).
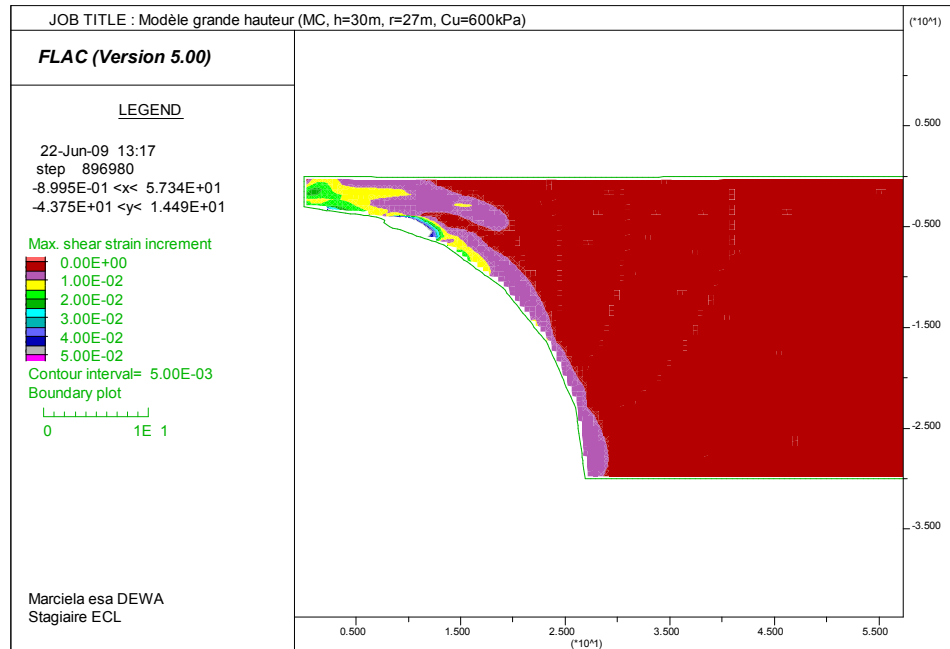
**Figure 70 Value γp refined Model MC great height (*h=30m, r=27m, Cu=700kPa*) (γpmax = 50%)**
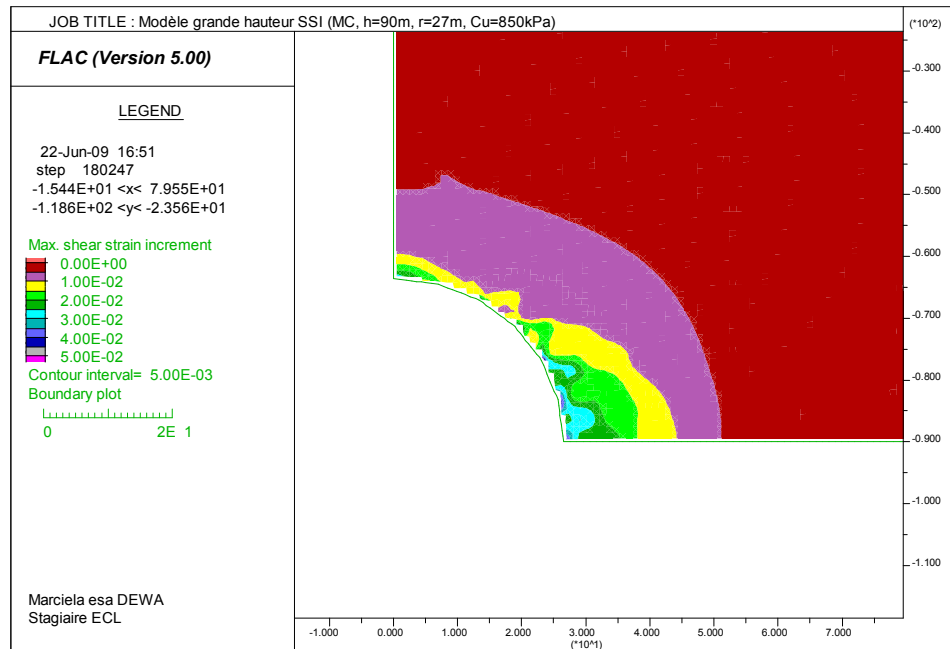
Figure 71 Value γp refined and zoomée - Model MC great height (*h=90m, r=27m, Cu=850kPa*)
**(γpmax = 5%)**
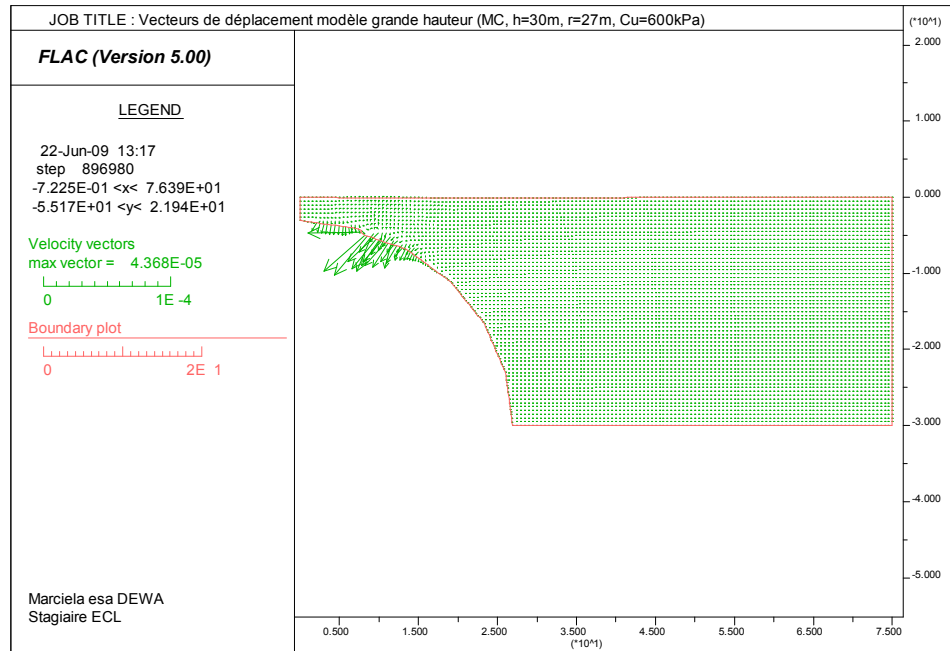
**Figure 72 Vectors of displacement models great height (*MC, h=30m, r=27m, Cu=700kPa*)**
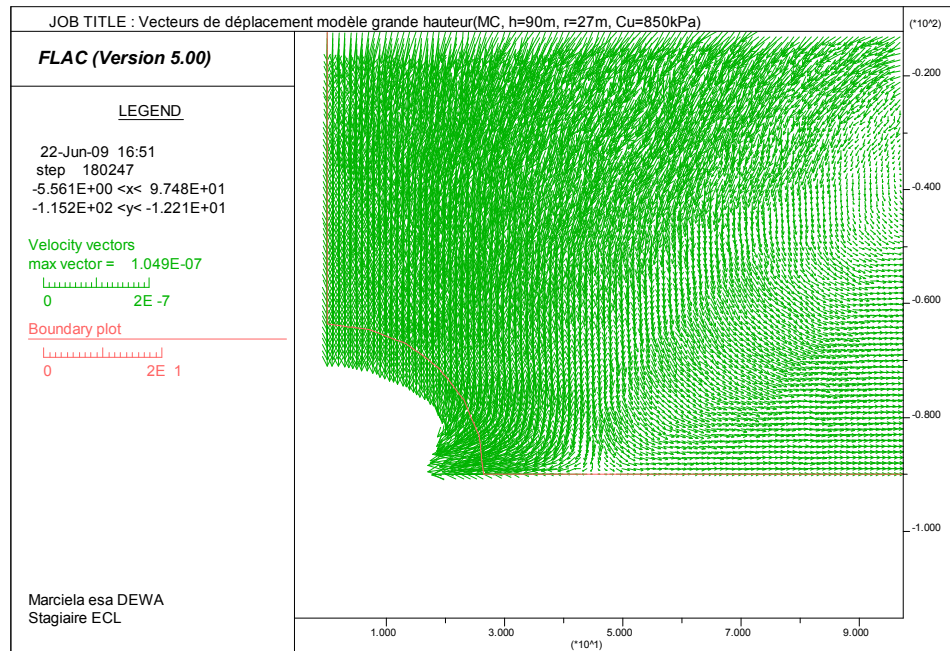
**Figure 73 Refined vectors of displacement model MC great height (*h=90m, r=27m, Cu=850kPa*)**
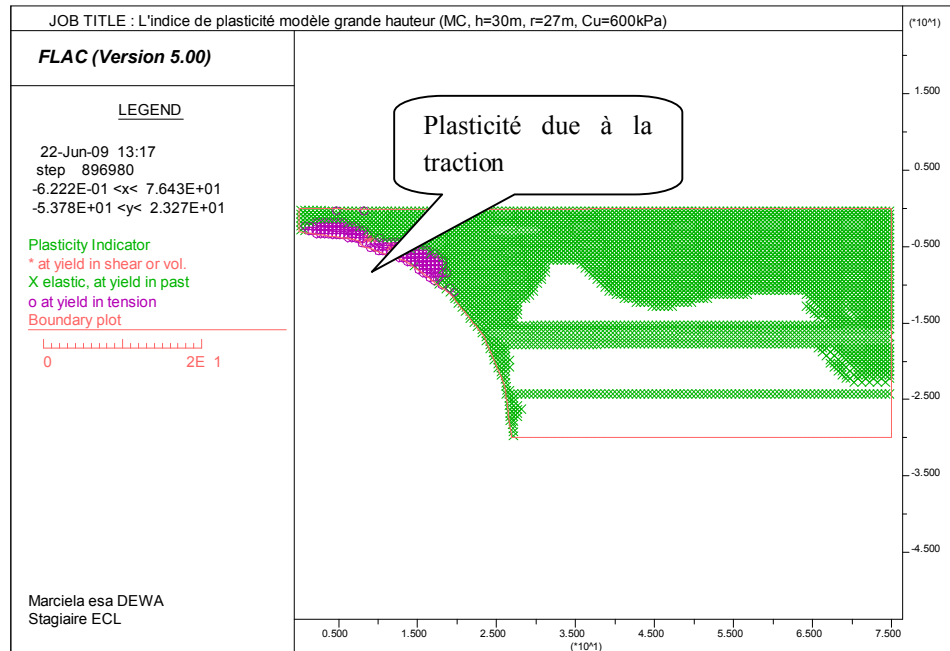
**Figure 74 Index of plasticity model MC, great height (*h=30m, r=27m, Cu=700kPa*)**
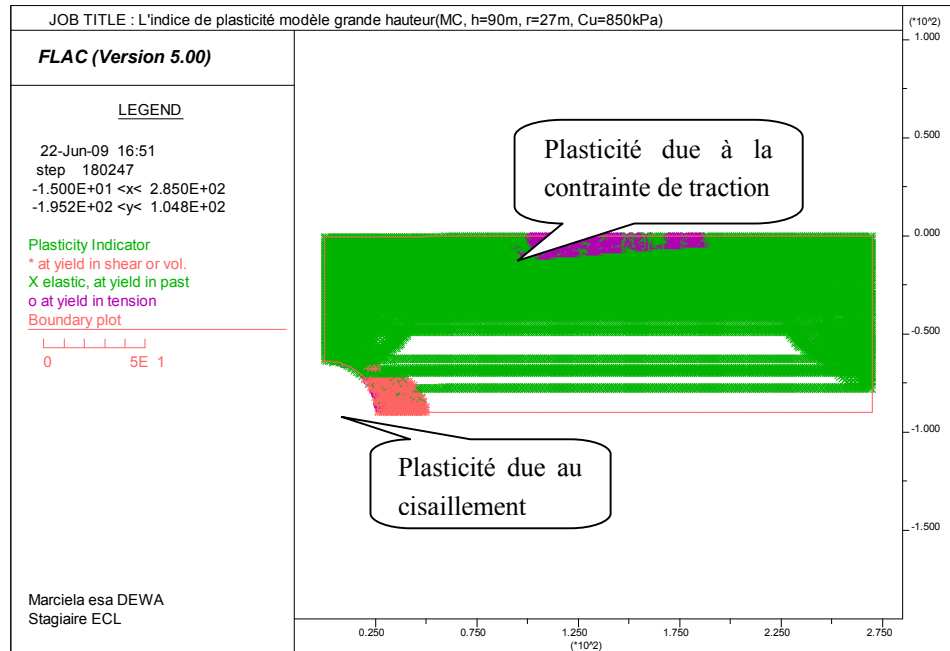
Figure 75 Index of plasticity model MC, great height (*h=90m, r=27m, Cu=850kPa*)

To facilitate the analysis, we put the results by the two heights of the earth dam in a curve (R - γp) while taking for all the two cases *Cref=5000kPa*.

Comparaison du modèle MC (r=27m)
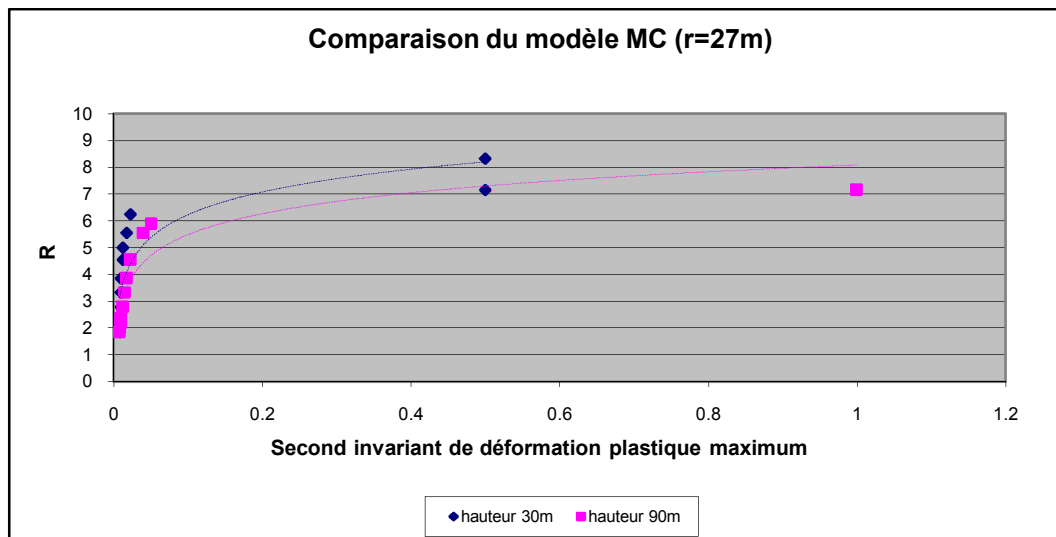
Figure 76 Comparison models great height with circular cavity of27 m (*MC*)

We note that the earth dam of 30m (with cavity of 27m) has almost the same number of stability as the earth dam of 90m (cavity of 27m) (see Figure 76). When the cavity is close to surface, plasticity due to the force with the traction is formed (Figure 74) which involves the system towards the rupture.

From Figure 69 we note that the earth dam having a height of 90m has a number of stability lower than the other earth dams (10m & 30m). What means that the height of earth dam also exploits the criterion of collapse. To check this assumption, let us take several cases: first of all models with a cavity of 18m (for the earth dams having a height of 30m and 90m).

Comparaison du modèle MC (r=18m)
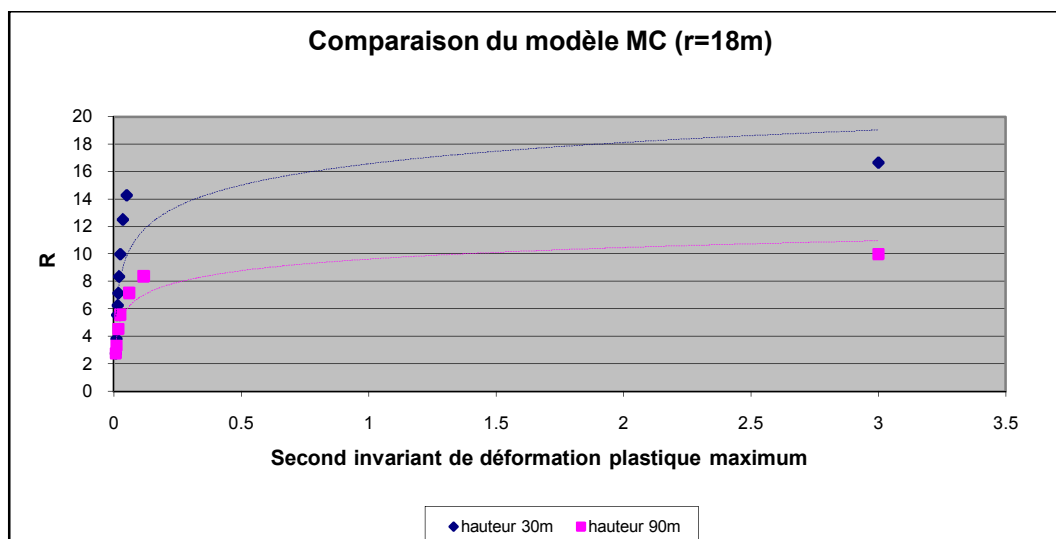
Figure 77 Comparison models great height with circular cavity of18 m (*MC*)

For the cavity of 9m, we use the following heights of earth dam (10m, 30m, and 90m),
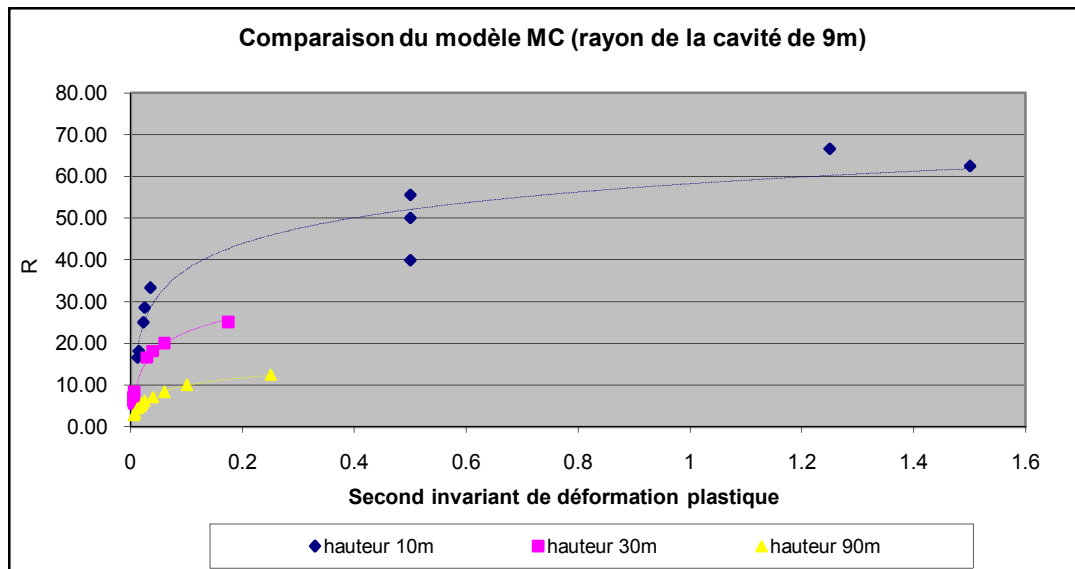
Figure 78 Comparison models great height with circular cavity of9 (*MC*)

For the cavity of 1m, we also use the three models,
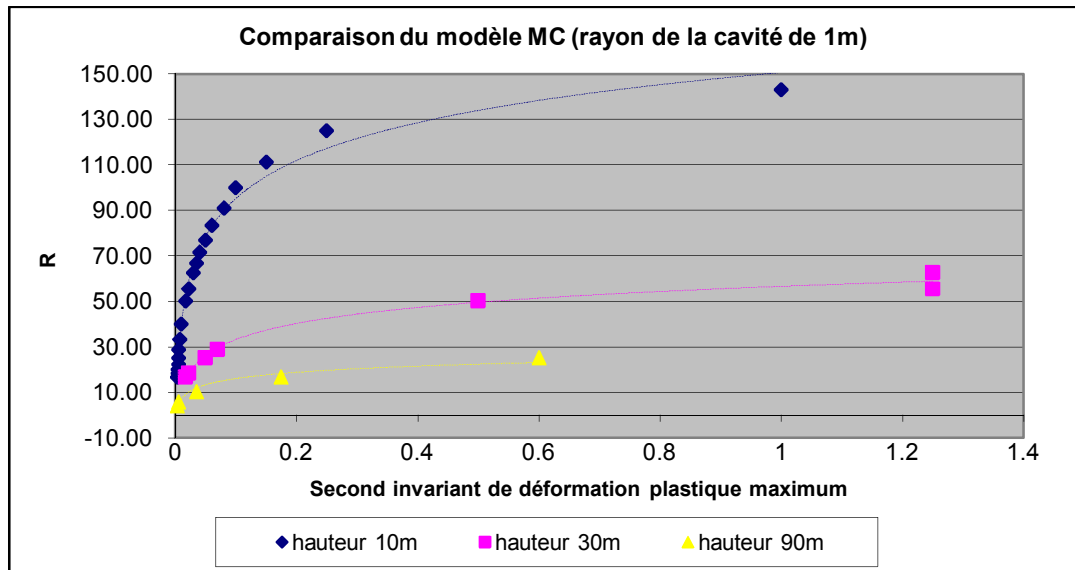
Figure 79 Comparison models great height with circular cavity of1 (*MC*)

We find that the height also plays an important component for the criterion of collapse. This assumption is ensured by the curve γ^p - R shown by Figure 76, Figure 77, Figure 78, and Figure 79 where more the earth dam is high (the height is large), plus $\underline{R_{ult}}$ is weak (large *Cu-ult*).

4.2 Analyze for Model of Mohr Coulomb with softening

To finish the part of numerical model, we use the Mohr Coulomb Model with softening which approaches the real case of the soil. The results are shown in Table 18 and Table 19,

Table 18 Model Radoucissant 1 (height of 10m) (*Cref=5000kPa*)

Height of the Model - h (m)	10			
Rayon - r (m)	1	3	5	9
Maximum coefficient of reduction - R_{max}	6.10	4.90	4.30	2.30
Limiting cohesion - C_{lim}; γ^p=5% (kPa)	95	140	170	260
Ultimate cohesion - C_{ult} (kPa)	81	102	116	217
γ^p_{max} (%)	100.00	70.00	200.00	150.00

Table 19 Model Radoucissant 2 (height of 10m) (*Cref=5000kPa*)

Height of the Model - h (m)	10			
Rayon - r (m)	1	3	5	9
Maximum coefficient of reduction − R_{max}	89	73	69	40
Limiting cohesion - C_{lim}; γ^p=5% (kPa)	75	90	100	190
Ultimate cohesion - C_{ult} (kPa)	56	68	72	125
γ^p_{max} (%)	120.00	125.00	200.00	175.00

We also made this model for an earth dam of great height. In fact, the radoucissant model1 is a preliminary one. It gives values of C_{u-lim} and C_{u-ult} that rather pessimists. We then use another model with residual parameters, in particular the natural angle of repose which starts to Figure on the model radoucissant 2.

Table 20 Model Radoucissant 1 (height of 90m) (*Cref=5000kPa*)

Height of the Model - h (m)	90				
Rayon - r (m)	1	9	18	54	81

Maximum coefficient of reduction - R_{max}	17.50	11.00	7.00	3.10	1.75
Limiting cohesion - C_{lim}; γ^p=5% (kPa)	800.00	875.00	2000.00	1700.00	10000
Ultimate cohesion - C_{ult} (kPa)	286	455	714	1613	2857
γ^p_{max} (%)	125.00	100.00	60.00	60.00	70.00

Table 21 Model Radoucissant 2 (height of 30m) (*Cref=5000kPa*)

Height of the Model - h (m)	30				
Rayon - r (m)	1	3	9	18	27
Maximum coefficient of reduction - R_{max}	35	33	25	16.5	7.5
Limiting cohesion - C_{lim}; γ^p=5% (kPa)	200	225	300	375	900
Ultimate cohesion - C_{ult} (kPa)	143	152	200	303	667
γ^p_{max} (%)	300	125	100	200	80

Table 22 Model Radoucissant 2 (height of 90m) (*Cref=5000kPa*)

Height of the Model - h (m)	90						
Rayon - r (m)	1	5	9	18	27	54	81
Maximum coefficient of reduction - R_{max}	23	19	11.5	8.5	7	3.3	2.25
Limiting cohesion - C_{lim}; γ^p=5% (kPa)	450	650	700	800	900	1600	4500
Ultimate cohesion - C_{ult} (kPa)	217	263	435	588	714	1515	2222
γ^p_{max} (%)	250	150	150	100	200	200	80

For the analysis, let us take the case of a earth dam with a cylindrical cavity of 5m,
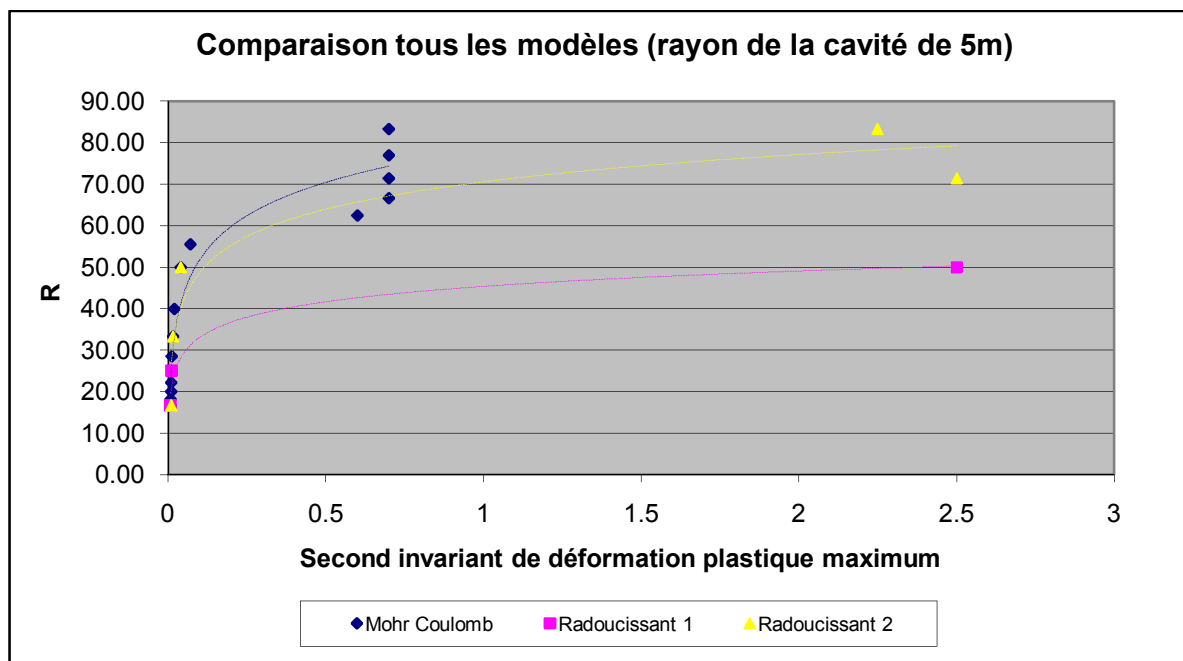
Figure 80 Result of the model radoucissant 1 & 2, and Mohr Coulomb (*circle, r=5m*) (*Cref=5000kPa*)

On the curve (Figure 80), We note that the two models radoucissant are less stable than the Mohr Coulomb Model. If we take the tendencies of the models of Mohr Coulomb and radoucissant 2, the two models give close results. It still remains to make a more detailed analysis of the process of collapse.

We compare the results of the models radoucissant obtained with the results of Mohr Coulomb on the following images,
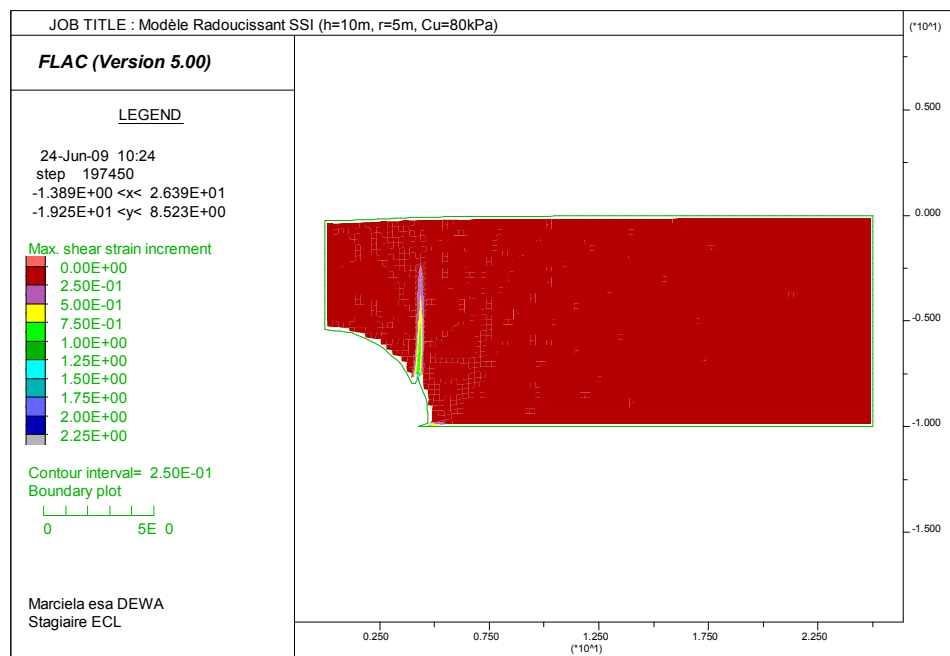
Figure 81 Value γp - Model Radoucissant 1 (*h=10m, r=5m, Cu=80kPa*)
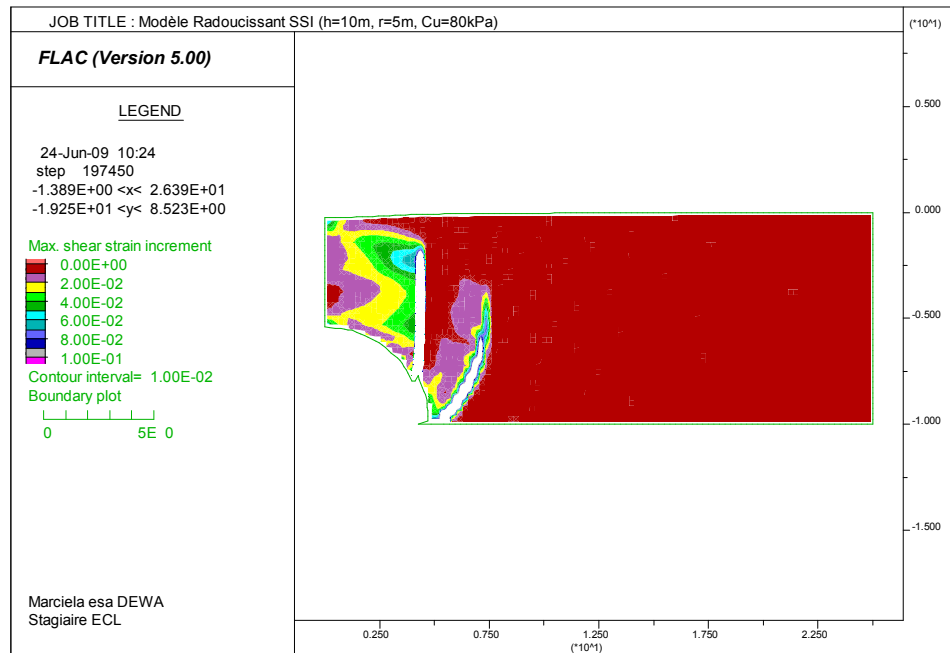
Figure 82 Value γp refined - Model Radoucissant 1 (*h=10m, r=5m, Cu=80kPa*)
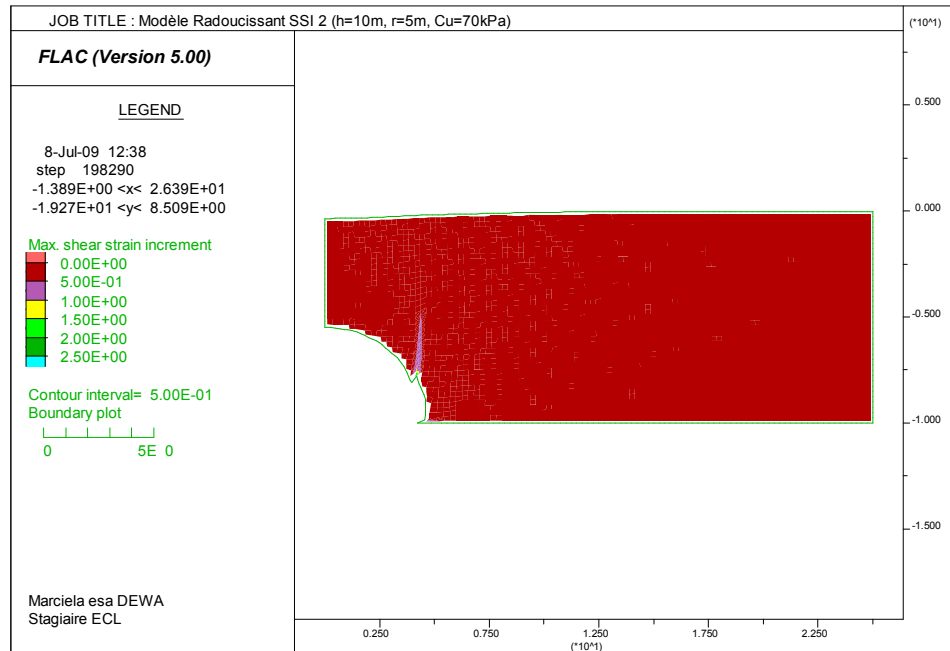
Figure 83 Value γp - Model Radoucissant 2 (*h=10m, r=5m, Cu=70kPa*)
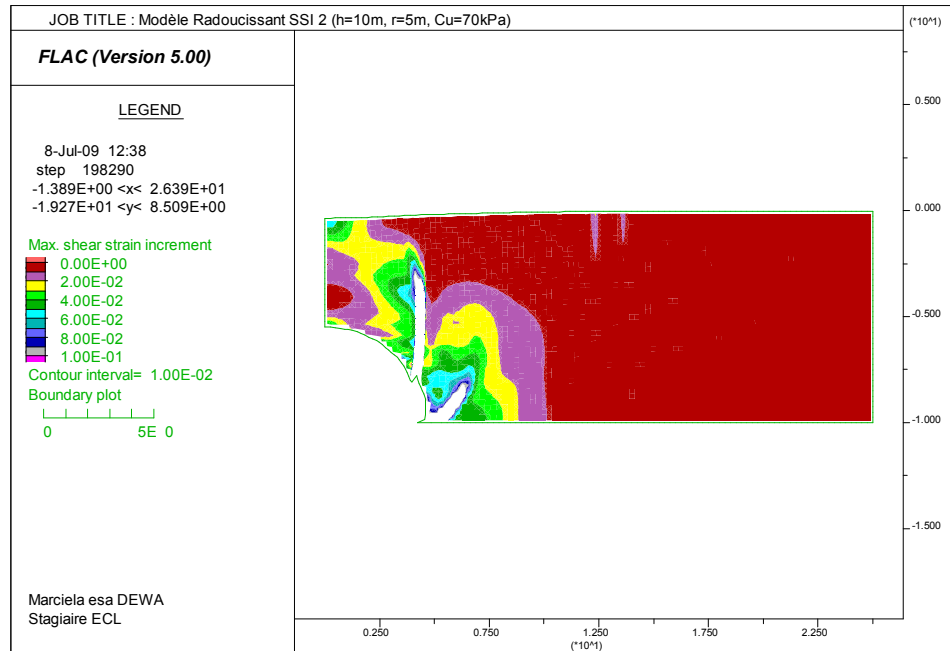
Figure 84 Value γp refined - Model Radoucissant 2 (*h=10m, r=5m, Cu=70kPa*)
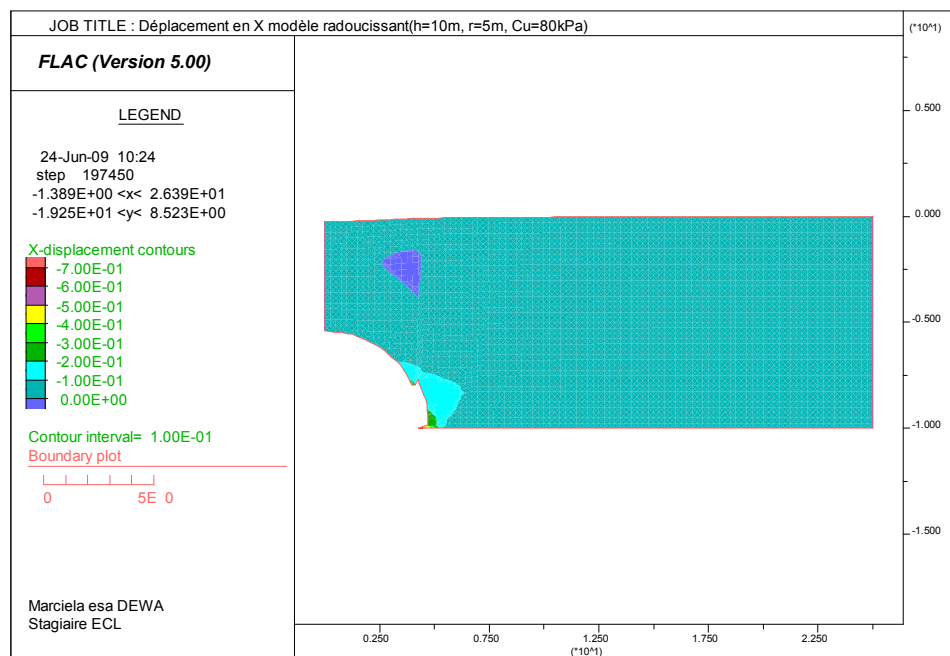
**Figure 85 Displacement in X model radoucissant 1 (*h=10m, r=5m, Cu=80kPa*)**
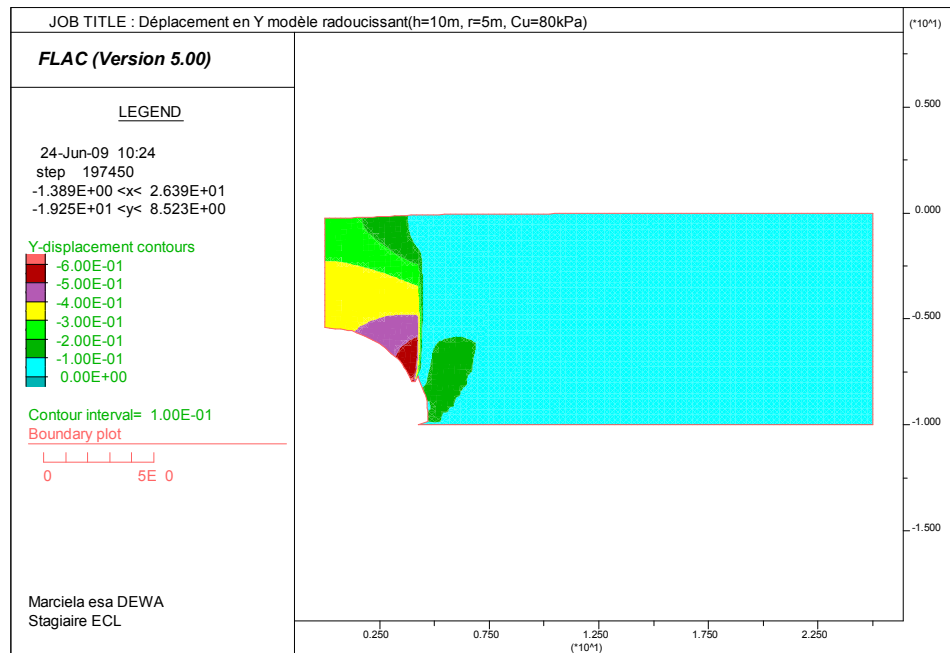
**Figure 86 Displacement in Y model radoucissant 1 (*h=10m, r=5m, Cu=80kPa*)**
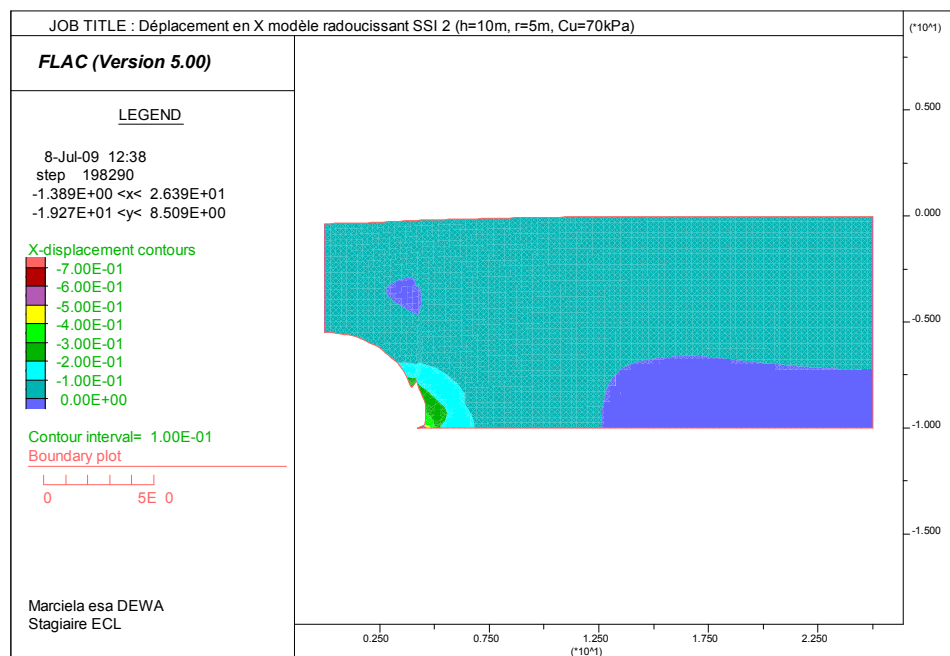
Figure 87 Displacement in X model radoucissant 2 (*h=10m, r=5m, Cu=70kPa*)
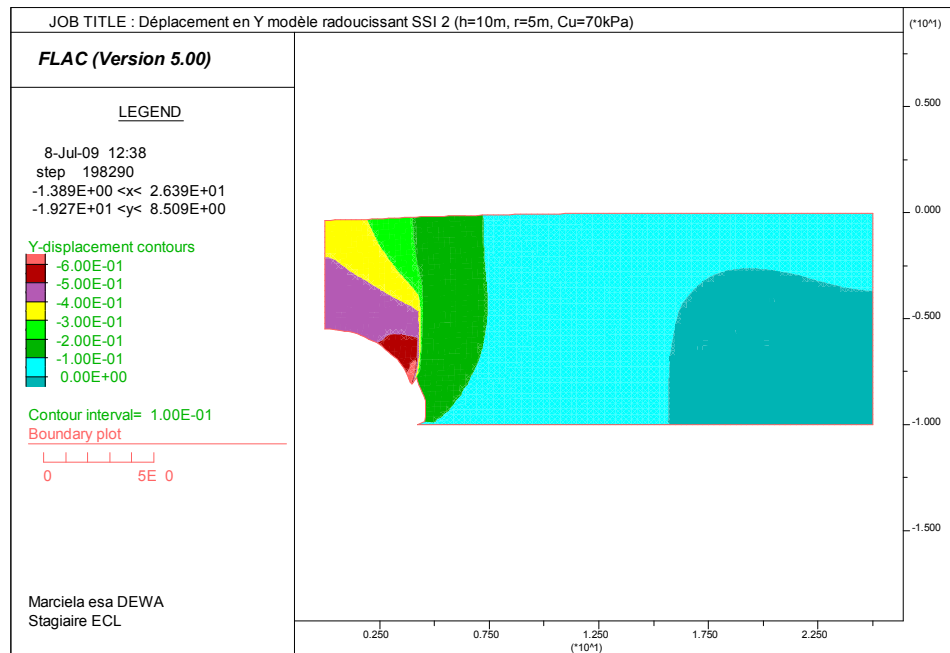
Figure 88 Displacement in Y model radoucissant 2 (*h=10m, r=5m, Cu=70kPa*)
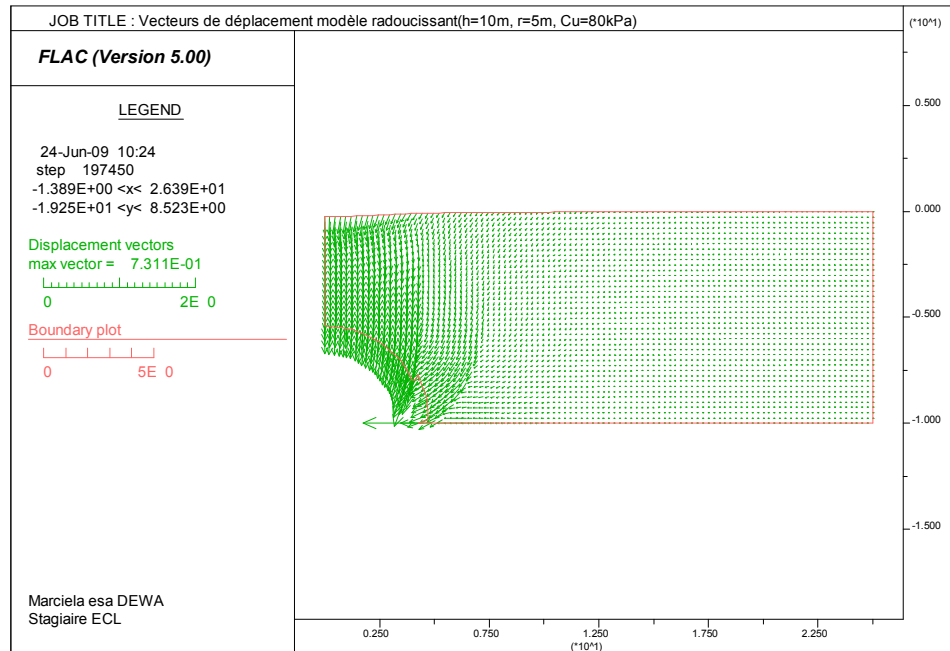
**Figure 89 Vectors of model displacement radoucissant 1 (*h=10m, r=5m, Cu=80kPa*)**
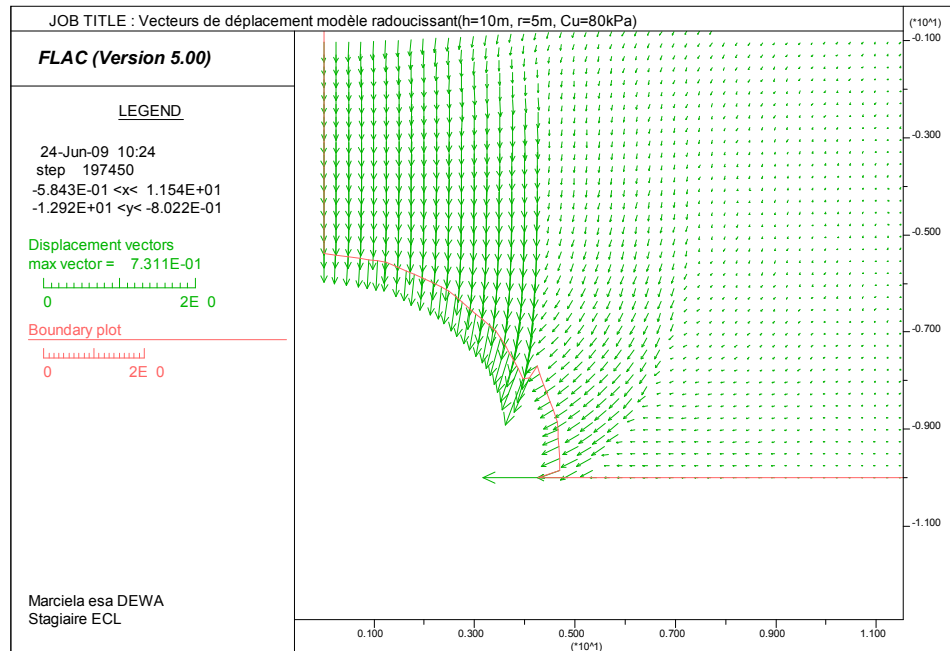
**Figure 90 Zoom of Vectors of displacement model radoucissant 1 (*h=10m, r=5m, Cu=80kPa*)**
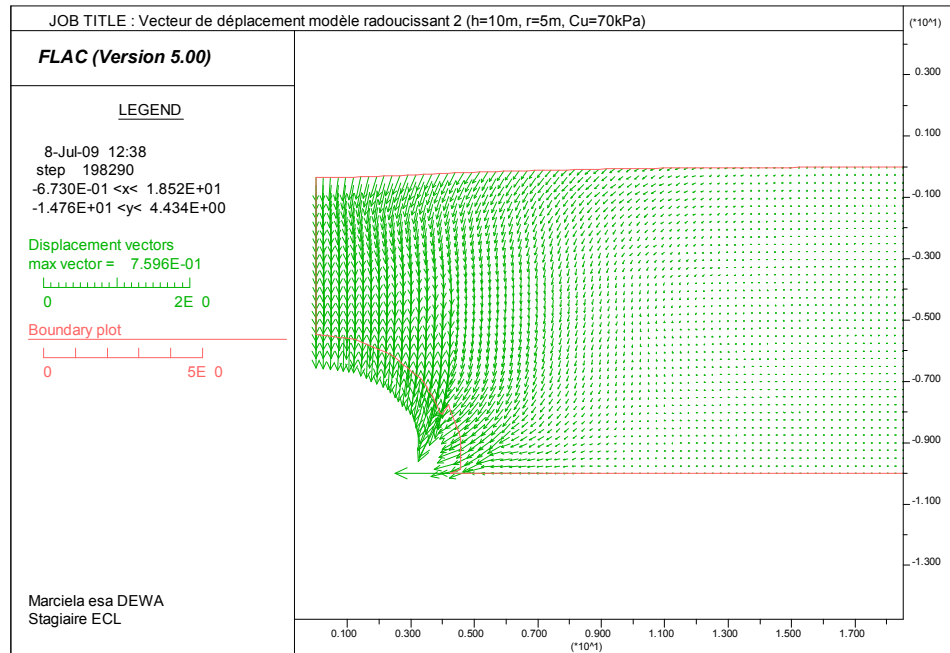
**Figure 91 Vectors of displacement model radoucissant 2 (*h=10m, r=5m, Cu=70kPa*)**
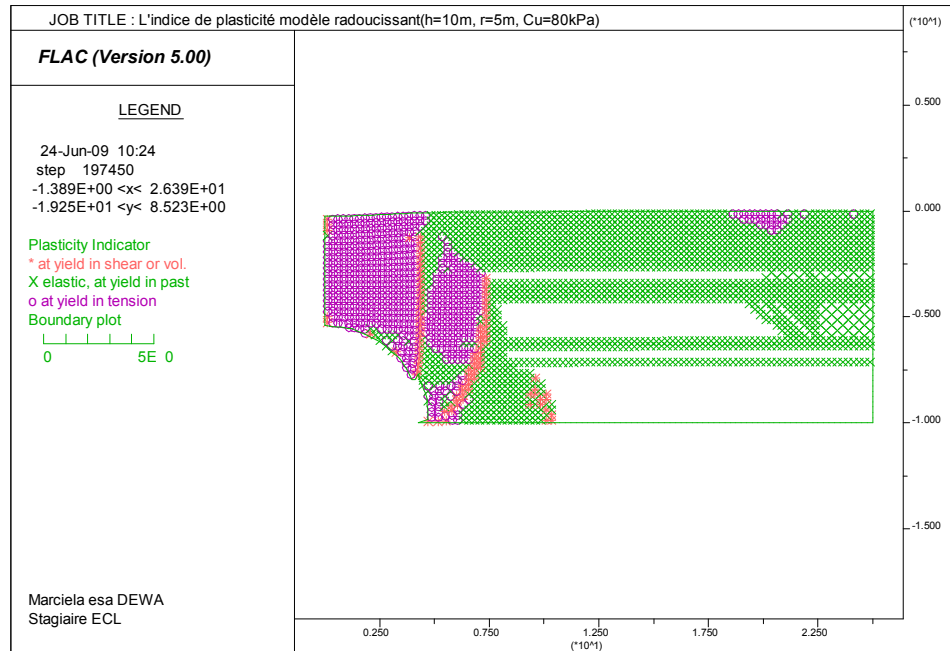
**Figure 92 Index of plasticity model radoucissant 1 (*h=10m, r=5m, Cu=80kPa*)**
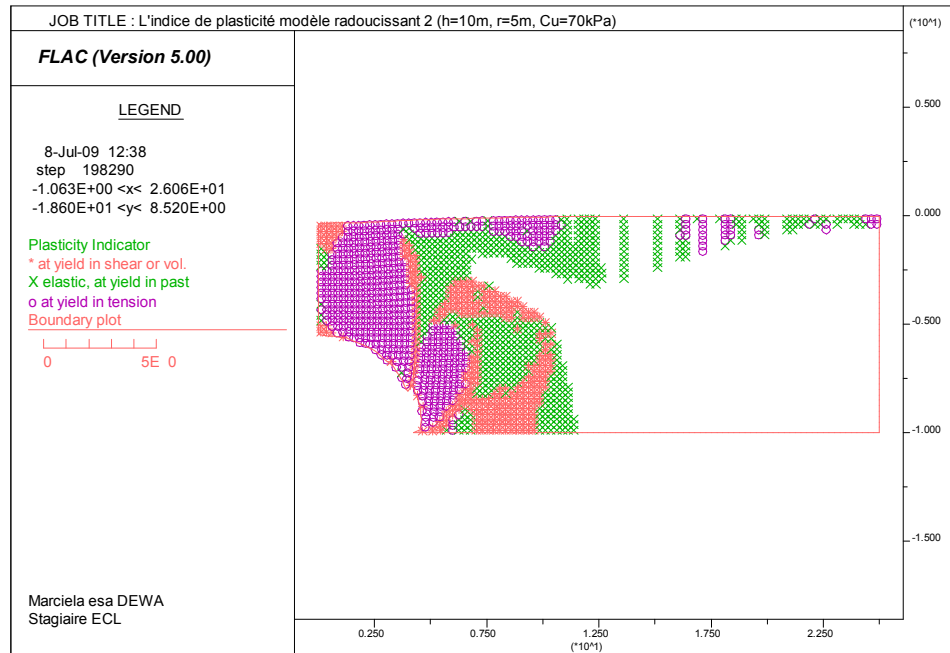
Figure93 Index of plasticity model radoucissant 2 (*h=10m, r=5m, Cu=70kPa*)

The results for the models radoucissants seem very reasonable for collapse, considering the mode of rupture (Figure 90 and Figure 91). They locate the lines of rupture.

From the results obtained, we note that the Mohr Coulomb Model with radoucissant is preferable that the Mohr Coulomb Model normal. This result is also valid for the system great height (either more 10m; from here 30m and 90m).

So that we finish by the conclusion and the prospects, we compare all the results in only one chart (Figure 94).
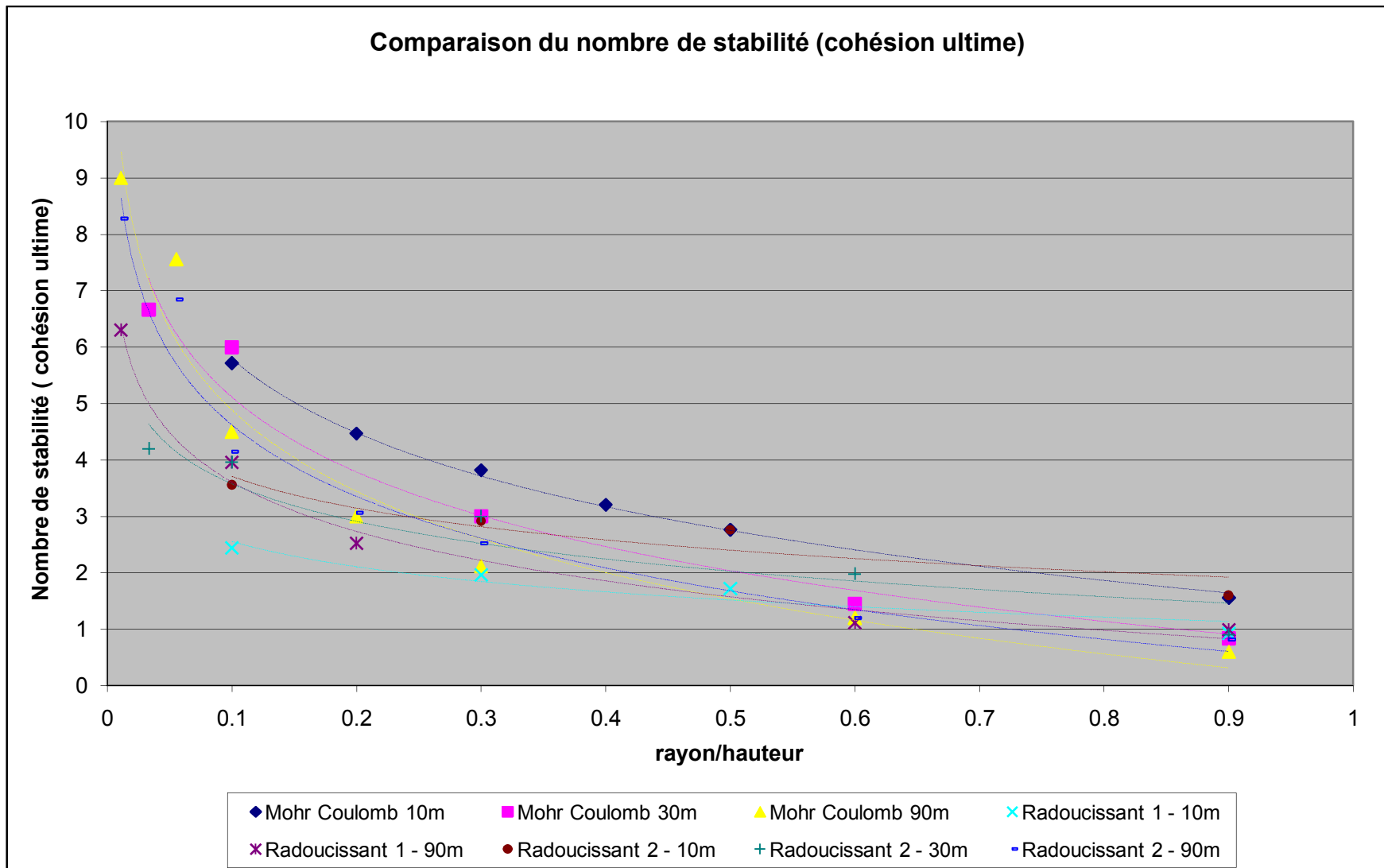
Figure 94 Comparison of the number of stability (all models; ultimate cohesion)

So that we can analyze, we compare the model by its height,
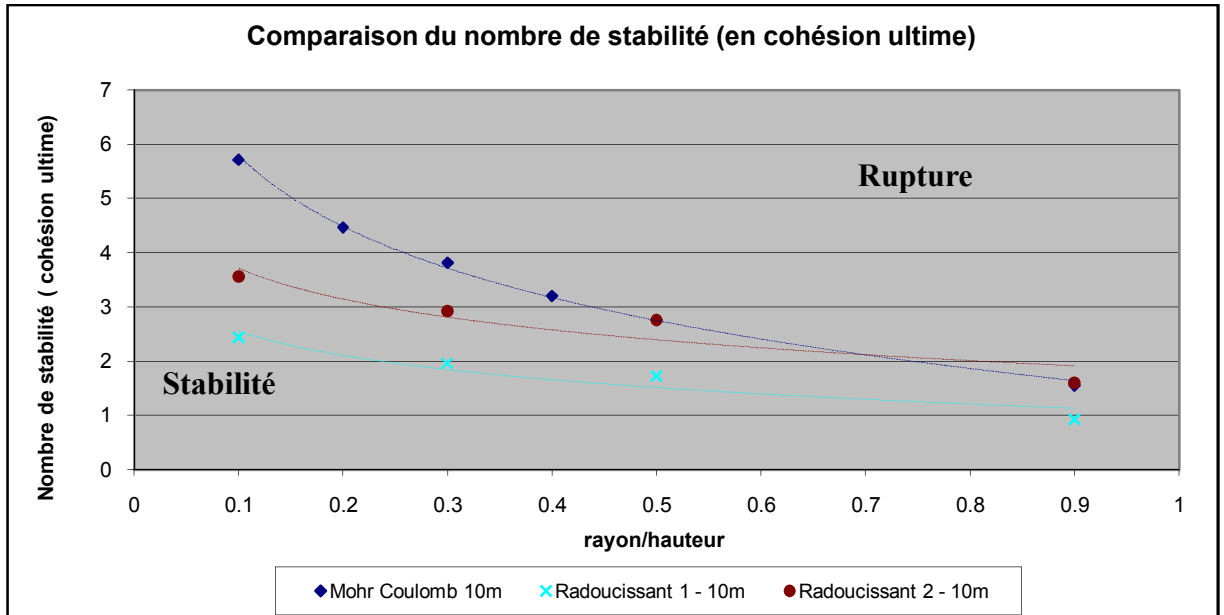
**Figure 95 Comparison of the number of stability for the model in low height (ultimate cohesion)**
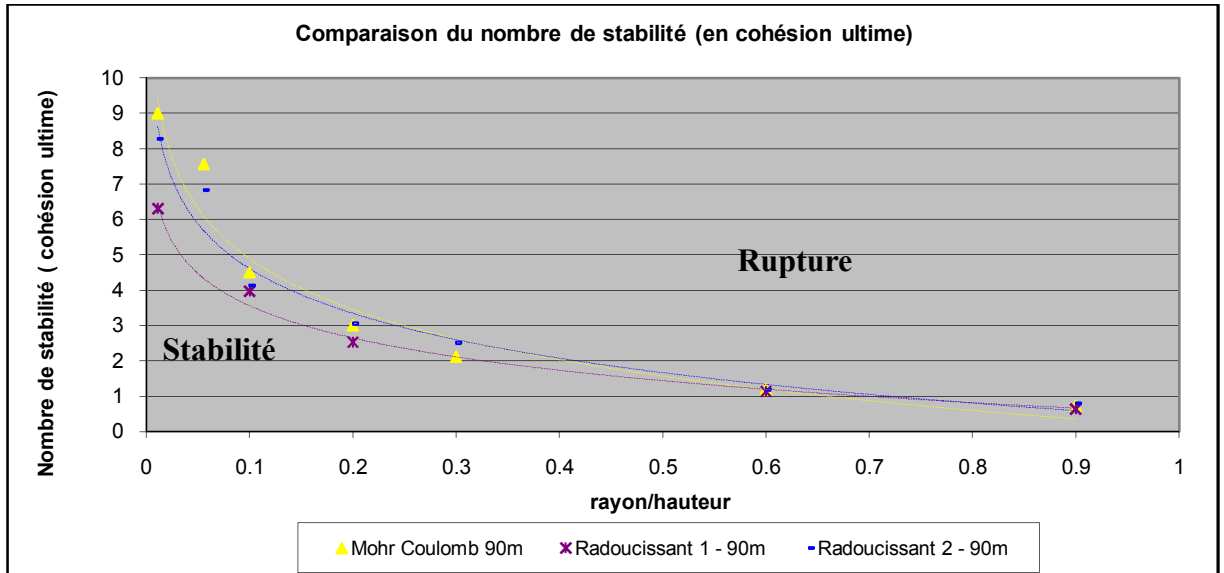
Figure 96 Comparison of the number of stability for the model in great height (ultimate cohe-sion)

The curves show that the three models have the same tendency of stability when the ratio of rayon/height is large. That is not the case by smaller ratios (Figure 95). This case is difficult to justify.

When the ratio of r/h is large (the cavity is close to surface), we find that the model radoucissant 2 is much more stable than the two other models. This phenomenon of collapse which occurs close to surface is made by the force with traction and the natural an-

gle of repose. When the cavity is close to surface, the zone of plasticity due to traction occurs, but having a mechanical property of the force to traction and the natural angle of repose, the model radoucissant 2 behaves better and has more resistance. This is valid only if the cavity close to surface.

With the model radoucissant 2, we also check the assumption of a mode of rupture in two times (Figure 89 and Figure 91). The vectors of displacements show us well that there is an effect of the widening of the breach when collapse evolves/moves. By using the image presentation of γ^p, we also note that the mode of rupture is done in two times. (Figure 82 and Figure 84)